THERMO-MECHANICAL ANALYSIS OF POLYAMIDE BIOCOMPOSITES

A Thesis
Submitted to the Graduate Faculty
of the
North Dakota State University
of Agriculture and Applied Science

By

Jessica Lynne Lattimer

In Partial Fulfillment of the Requirements
for the Degree of
MASTER OF SCIENCE

Major Department:
Mechanical Engineering

December 2012

Fargo, North Dakota

North Dakota State University
Graduate School

Title

Thermo-Mechanical Analysis of

Polyamide Biocomposites

By

Jessica Lattimer

The Supervisory Committee certifies that this ***disquisition*** complies with North Dakota State University's regulations and meets the accepted standards for the degree of

MASTER OF SCIENCE

SUPERVISORY COMMITTEE:

Dr. Chad Ulven
Chair

Dr. Bret Chisholm

Dr. Bora Suzen

Dr. Xinnan Wang

Dr. Dean Webster

Approved by Department Chair:

12/19/12
Date

Alan Kallmeyer
Signature

ABSTRACT

Biobased fillers in thermoplastics have seen increased usage over the last several years. The increased usage of biobased fillers follows the ever-increasing thrust to reduce petroleum and synthetic petrochemical product consumption. Biocomposites made from polyolefin matrices have shown improved elastic moduli with moderate impact on strength. For engineering thermoplastics, the increased processing temperatures lead to degradation of the biomass, often detrimental for the mechanical performance. The goal of this work was to evaluate the effectiveness of agricultural byproducts as fillers in polyamides, while minimizing the effects of increased processing temperatures. Torrefaction has been identified as an effective means of preparing biomass for introduction into polyamide. Polyamide biocomposites were produced and shown to have comparable mechanical properties to the neat matrix. Torrefied biomass was shown to produce tensile strengths within 70% of the neat matrix, increase elastic modulus by 150%, flexural strength by 170%, and flexural modulus by 154%.

TABLE OF CONTENTS

LIST OF TABLES

LIST OF FIGURES

CHAPTER 1. INTRODUCTION

Over the last decade the use of biobased materials as fillers in thermoplastics has seen a remarkable increase. The low cost to density ratio coupled with improved mechanical properties and processing conditions, have led to the increased acceptance of natural fibers as replacements for traditional synthetic fibers [1–6]. It is well known from previous work that adding natural fiber reinforcements to commodity polyolefin matrices (i.e. polyethylene, polypropylene, etc.) will in general increase the elastic modulus, decrease the tensile strength, increase the flexural performance, and decrease the impact resistance of the material. By adding reinforcements to the neat matrix, these rigid impurities in the material prevent the polymer chains from sliding past one another, thus causing an increase in modulus, a decrease in tensile strength, and induced brittle failure. The filler can be considered as the impurities in the biocomposite because of a lack in interfacial bonding between the filler and matrix. The lack of interfacial bonding comes from the mismatch in polarities between the matrix and filler; the matrix generally being hydrophobic and the filler being hydrophilic. However, these imperfections are the cause of increased elastic modulus by impeding the molecular chain movement within the polymer. They are also the cause of increased flexural performance and decreased impact resistance. In polyolefin matrices it has been determined the use of a compatibilizer can aid in improving the interfacial bond between filler and matrix. While the focus has thus far been on producing biobased composites out of commodity polyolefins or bio-derived resins, little work has been done in the realm of engineering thermoplastics [1-2, 4–7].

1.1. Polyamide Composites

For many years the increased rigidity, good resistance to creep, improved wear resistance, and increased heat deflection temperatures of polyamide composites have been used to replace metals in a vast array of applications. Due to the increased processing temperatures of polyamides only thermally stable fillers such as fiber glass, carbon fibers, and minerals have been used. Of all the fillers used in polyamide composites, fiber glass is the most common. It was estimated in 2003 that 200,000 tons of glass filled polyamides are used every year [8–9].

The fastest growing use of polyamides is accredited to the automotive industry. Since the discovery of polyamides in 1939 the automotive industry has used it to replace weight expensive metals parts, with an immediate implementation for self-lubricating bearings after its introduction at that year's World's Fair. Initially designers limited the use of polyamides to non-critical components due to a lack of information on how polyamides performed in harsh environmental conditions [10–11].

The 1960s brought about an increased use of polyamides in cars, with an average of 0.4 pounds of polyamide per vehicle. The introduction of glass and mineral filled polyamides around 1968 changed the mindset of designers, who began designing polyamide radiator and fuel system components. An enhanced understanding of the high temperature performance and chemical resistance of polyamides along with government regulations for pollution control, pushed the consumption of polyamides and polyamide composites even higher in the 1970s. An average of 2 pounds of polyamide was in every car. It wasn't until the 1980s that polyamides and their composites were really trusted for high performance components, such as air intake manifolds, and was consistently used across all lines of

vehicles. The polyamide and polyamide composite content of cars jumped to an average of 8.8 pounds by 1995, including general acceptance of polyamide air and cam manifolds, and the United States automotive industry alone consumed 212 million pounds polyamides. This wide acceptance of polyamides in vehicle design made it the largest used engineering thermoplastic in the automotive industry. By 2000 every car contained on average 11.06 pounds of polyamides and polyamide composites an increase of 30% from the introduction of polyamides automotive parts in 1960 [10–11].

1.2. Polyamide Biocomposite Production

For engineering thermoplastics, the increased processing temperatures cause degradation of the natural fiber. This degradation is the breakdown of hemicellulose (220 - 320 °C), fats, residual waxes, etc. leaving behind the cellulose and lignin that do not fully degrade at these temperatures [12]. While the natural fiber does not degrade completely, volatiles deposited on the fiber surface are enough to hinder mechanical performance of the composite. One method of preventing the degradation of biobased fillers is to decrease the amount of time the filler is exposed to the increased temperatures. There have been several attempts at nylon biocomposites in which the biobased fillers were introduced in a manner that minimized the exposure time. Compression molding with a 2.5 minute cycle time to minimize the degradation of the filler and an extrusion process that introduce filler down-stream just before the die are all methods of reducing filler degradation [1, 3].

The introduction of Curauá fibers, the leaves from a tropical fruit much like the pineapple, during a twin screw extrusion process was shown to be successful in reinforcing polyamide 6 when the fibers were introduced just before the die. An intermeshing co-

rotating screw was used for this work and a temperature profile from feeder to die of 215, 220, 225, 230 °C was used. A fiber loading of 20 wt% was achieved during this extrusion process, however, the tensile and flexural properties fell short of the traditional glass or talc filled polyamide 6 (PA6) composites. Table 1.1 shows mechanical properties of the 20 wt% filled polyamide composites. The tensile strength of the Curauá filled polyamide displays an 18% drop below the traditional glass filled polyamide. However the Curauá filler does show improved tensile strength over the talc composite. Thus the Curauá filled polyamide biocomposites are viable replacements for certain applications where glass or talc filled composites are currently used [3].

Table 1.1: Tensile, Flexural, and Density Comparison of 20 wt% Curauá, Glass, and Talc Filled Polyamide 6 Composites [3]

Filler	Tensile Strength (MPa)	Tensile Modulus (GPa)	Flexural Strength (MPa)	Flexural Modulus (GPa)	Impact Toughness (kJ/m^2)	Density (g/cm^3) ±0.01
PA6	63 ± 1	1.3 ± 0.1	95 ± 1	2.2 ± 0.1	10 ± 1	1.13
Curauá	83 ± 3	5.1 ± 0.4	116 ± 2	3.7 ± 0.1	9 ± 2	1.18
Talc	73 ± 1	6.7 ± 06	114 ± 2	4.4 ± 0.1	9 ± 2	1.27
Glass	101 ± 1	6.5 ± 0.5	160 ± 5	5.0 ± 0.1	7 ± 1	1.27

A second method of limiting natural fiber exposure during processing is to utilize compression molding. Polyamide 6 fibers and wood fibers were combined and pressed into rectangular plaques using 50 kN of force at a temperature of 230 °C. The composite plaques were held under pressure at temperature for 2.5 minutes. Filler loadings of 2.5, 5, 7.5, and 10 wt% were achieved using the compression molding process. Table 1.2 summarizes the tensile properties measured from the compression molded specimens. It can be seen from the table that the incorporation of wood fiber into the polyamide matrix increased the tensile modulus by as much as 42% over the neat polyamide 6. The tensile strength also showed improvement with added wood fiber by as much as 53% [1].

Table 1.2: Tensile Properties of Compression Molded Polyamide Wood Composites [1]

Wt%	Tensile Strength (MPa)	Tensile Modulus (GPa)
0	30	1.9
2.5	46	3
5	40	2.6
7.5	31	2.4
10	34	2.7

In both the Curauá and wood fiber studies, the biocomposites produced showed improvements on both tensile and flexural properties. In a polyolefin biocomposite the tensile strength generally decreases due to the poor fiber-matrix interactions. For a polyamide based biocomposite the interfacial bond between fiber and matrix is stronger. Polyamides are more hydrophilic as compared to polyolefins which make their inherent compatibility with very hydrophilic biomass better. Without the need of an added compatibilizer to strengthen the fiber-matrix bond polyamide biocomposites are more economically appealing than polyolefin biocomposites [1, 3].

While the cost savings of replacing an expensive plastic such as polyamide with inexpensive fillers is appealing, moisture uptake is a concern. The hydrophilic nature of polyamide, while good for aiding in fiber-matrix bonding, is detrimental to maintaining mechanical integrity in harsh environmental conditions. Moisture is absorbed through the amorphous regions of polyamides and begins to modify the structure. Interchain hydrogen bonds begin to weaken as a result of absorbed moisture. This softening of bonds allows increased chain movement in the polymer, thus decreasing glass transition temperature and decreasing mechanical integrity. Figure 1.1 shows the chemical structure of polyamide 6 and 6,6. The interaction of water molecules and polyamides occurs between the carbon oxygen double bonds and nitrogen hydrogen bonds where hydrogen bonding occurs between polymer chains. This hydrogen bond is what limits the chain movement in dry

polyamides. Figure 1.2 shows the interaction of water molecules in more detail, the red circles indicate the water molecules that have weakened the chain to chain hydrogen bonding [13]. For a greater acceptance of polyamide biocomposites, the issues of fiber degradation and moisture absorption need to be addressed.

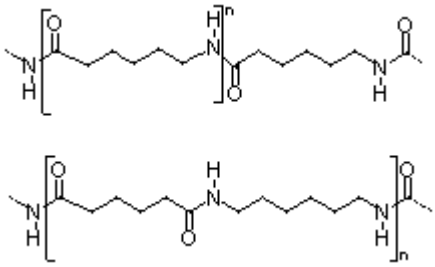

Figure 1.1: Chemical structure of polyamide 6 (top) and polyamide 6,6 (bottom).

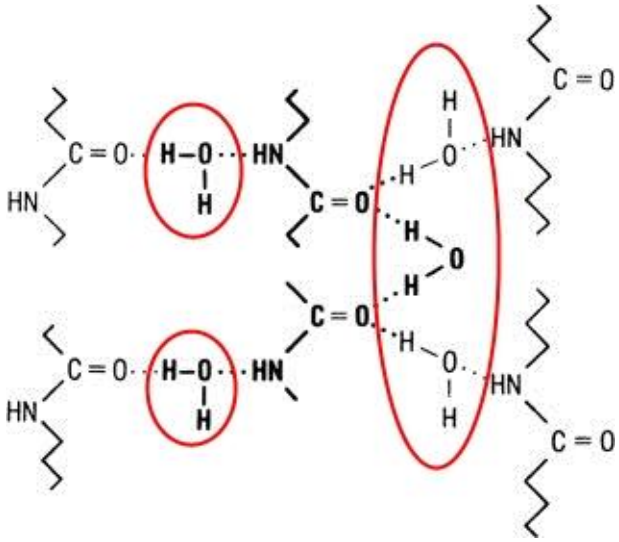

Figure 1.2: The interaction of water in polyamides [13].

1.3. Chemically and Thermally Modified Fillers

Chemical modification of wood dates back to 1928 and is simply defined as covalently bonding molecules to reactive sites along the cell wall polymers of wood. While there is an array of chemicals suitable for chemical modification of wood fibers, the acetylation process using acetic anhydride is the most common. In 1928 the first acetylation of pine wood was performed with acetic anhydride and sulphuric acid catalyst to isolate lignin. The

acetylation of beach wood later in 1928 showed that through the isolation of lignin the hemicellulose present in the wood could be removed. Then in 1946 it was discovered that the acetylation of wood could prevent swelling during moisture absorption [14].

While the acetylation of wood has been well studied over the years the process can also be applied to many biobased fibers. Acetylation is a chemical reaction that replaces one hydroxyl group in the biobased fiber molecule with an acetyl group from the acetic anhydride. Figure 1.3 shows the chemical reaction between natural fibers and acetic anhydride. The acetylation process is very simple; fibers are washed in acetic anhydride while heat is applied then dried before being processed into biocomposites. As Figure 1.3 shows, the by-product of acetylation with acetic anhydride is acetic acid, a flammable irritant that has harmful vapors [14–18]. The addition of acetylated fiber has shown to improve the dimensional stability, hydrophobicity, and interfacial shear strength in polymer matrix biocomposites [15–18].

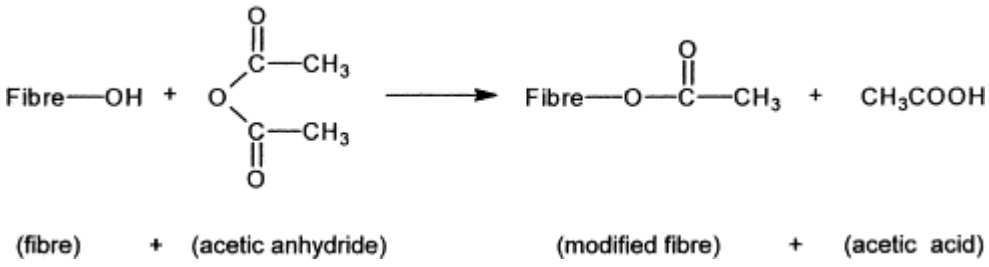

Figure 1.3: The chemical reaction that occurs during acetylation of natural fibers using acetic anhydride [18].

While acetylation will sufficiently modify the surface of natural fibers to improve mechanical performance over untreated fibers, the use of harsh chemicals can be undesirable. A more recent process known as thermal modification has shown to be promising at eliminating the need for harsh chemicals while maintaining the desired improvements of fiber modification. Thermal modification much like the acetylation

process is done at elevated temperatures, around 200 °C for several hours, but in an atmosphere low in oxygen content. At 140 °C the degradation of natural fibers begins to be significant when exposure times are lengthy. In an atmosphere low in oxygen the hemicellulose, and to a small extent the amorphous cellulose, begins to break down. It is not until the temperatures reach 230 °C that the amorphous cellulose decomposition becomes significant. Due to the low temperature of thermal modification the thermally stable crystalline cellulose will not see any structural changes. When added to polymer matrices, thermally modified fibers have been shown to improve the dimensional stability, hydrophobicity, and interfacial shear strength over untreated fibers [11, 12, 14]. However, as thermal modification is only conducted at 200 °C, well below the process temperatures of most engineering thermoplastics, a more aggressive method such as torrefaction must be employed before natural fibers can be introduced into engineering thermoplastics.

1.4. Torrefaction

Torrefaction, traditionally used to produce alternative energy sources, is a decomposition and densification process that removes low weight energy-light constituents from biomass. Three distinct phases are created during the torrefaction process: a solid carbonized mass, an acidic liquid phase, and syngas. One advantage of the solid by-product of torrefaction over untreated biomass, for the energy sector, is the production of a more homogeneous, dry lignocellulosic material high in energy content. Another advantage is the ability to store torrefied biomass for extended lengths of time without any concern of bacterial growth or biodegradation due to environmental exposure. The ability to store torrefied biomass for extended periods of time stems from the increased hydrophobicity of

the fiber. Although torrefaction of biomass has been studied extensively over the last several years, the exact chemical reactions occurring during the process are still unclear. It has been shown that the breakdown of hydroxyl groups on cellulose microfibrils is the cause of increased hydrophobicity [12], [20–25].

The solid by-product of torrefaction can be used in the traditional gasification or co-firing processes for electricity production, but its heating value is lower than that of traditional coal. However, it also has the potential to be used in biocomposite production with high temperature thermoplastics such as polyamide. The increased hydrophobicity being a potential solution for the moisture absorption issues discussed earlier with polyamide biocomposites. The syngas produced during torrefaction can potentially be burned to power the next torrefaction process making it self-sustaining after the initial torrefaction run.

As discussed with thermally modified fillers, natural fibers begin to significantly degrade at 140 °C when exposure times are lengthy. The major difference between the thermal modification and torrefaction is temperature range. Torrefaction is traditionally done in the range of 225-300 °C in an inert atmosphere for several hours. The length and temperature chosen for the process will determine the degree of torrefaction of the fibers. As with the thermal modification the hemicellulose, fats, waxes, and other low degradation point constituents within the fibers are driven off yielding a biomass consisting of mostly crystalline cellulose, degrading between 300–375 °C, and lignin, degrading slowly over 250–500 °C [15–16]. In the mild degradation during thermal modification the amorphous cellulose saw minor structural changes; torrefaction will degrade the amorphous cellulose to a higher degree and begin to mildly degrade the crystalline cellulose.

While certain constituents are being stripped form the biomass all together, the remaining constituents are undergoing some molecular changes. As the temperature at which torrefaction is conducted increases, the amount of char produced from the remaining lignin and cellulose also increases as seen in Figure 1.4. Part A of Figure 1.4 shows the chemical characteristics of the components within natural fiber and part B shows the components of the solid torrefaction by-product or char. There are four distinct char regions depending on the torrefaction temperature. Transition char results from the mildest torrefaction. In this region the lignin begins to de-polymerize, the amorphous cellulose sees significant degradation, crystalline cellulose begins to see molecular changes, and char begins to form. The next degree of torrefaction yields amorphous char. In this region the amorphous cellulose and lignin are completely degraded and very little crystalline cellulose remains. The most severe degrees of torrefaction occurring above approximately 400 °C have stripped all forms of cellulose and lignin from the fibers. At these temperatures turbostatic crystallites form and continue to grow with increased temperature, but the char does not reach the order or crystallinity of graphite [21].

As crystalline cellulose is the component within natural fibers that reinforces biocomposites, maximizing the survival of this component during torrefaction is critical to producing viable filler for polyamide biocomposites. For this reason the bulk of this work will focus on the production of transition char; more specifically the production of transition char that contains little to no hemicellulose. As it would be impractical to conduct the torrefaction of biomass for commercial composite production using thermal gravimetric analysis another method of determining the degree of torrefaction is needed.

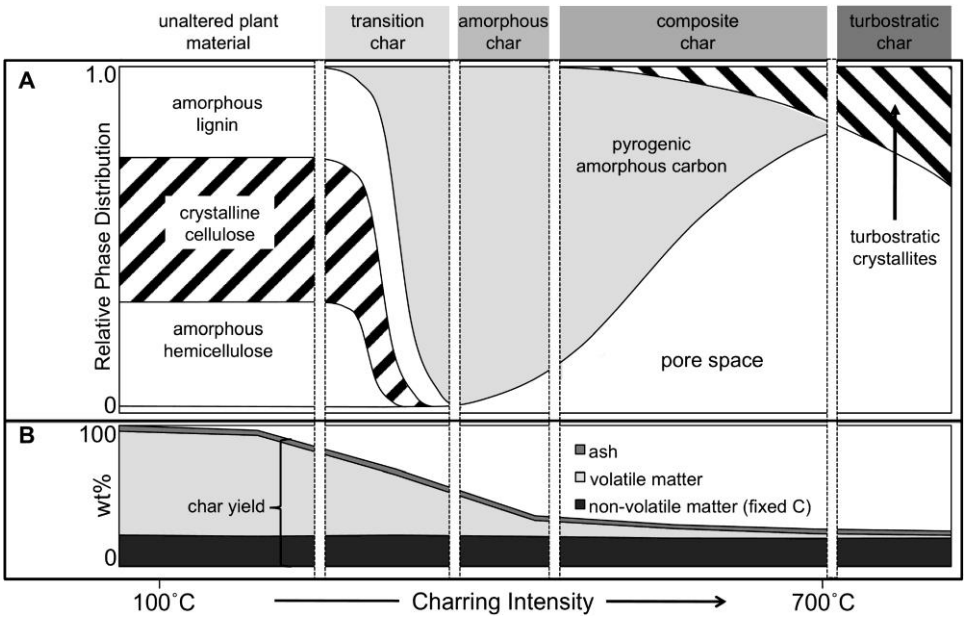

Figure 1.4: Char characteristics and constituent break down at varying temperatures of torrefaction measured by thermal gravimetric analysis [21].

Knowing which of the constituents present in a biomass feed stock will be stripped form the fibers during torrefaction will indicate how much mass should be lost during the process. Calculating the percent yield of a torrefaction process will indicate the degree to which it was torrefied. This first requires knowing the break down by mass percentage of the various constituents present in biomass feedstock. There are many ways of determining the constituent makeup of a biomass feedstock, for this work wet chemical analysis was employed. As lignin and cellulose are the primary constituents remaining after torrefaction, the addition of their mass content will indicate how much of the biomass weight should remain after a successful process. Fourier transform infrared spectroscopy (FTIR) can also be used to indicate the changes to chemical bonding due to the torrefaction process.

CHAPTER 2. OBJECTIVES

Biobased fillers in thermoplastics have seen a remarkable increase in usage over the last several years. The increased usage of biobased fillers follows the ever-increasing thrust to reduce petroleum and synthetic petrochemical product consumption [1–5]. Biocomposite research has been well established in polyolefins and thermoset matrices. However, the incorporation of biomass into engineering thermoplastics is a challenge. The increased processing temperatures lead to filler degradation, hindering the mechanical performance of the biocomposite. By pretreating the filler, the constituents with degradation temperatures below the processing temperatures of engineering thermoplastics can be modified. The first objective of this work is to identify a viable method of pretreating natural fibers for introduction into engineering thermoplastics. The second objective is to produce and evaluate the effectiveness of the pretreated fiber as reinforcement in engineering thermoplastic based biocomposites.

The automotive industry, the single largest consumer of polyamides, is becoming a proponent of greater utilization of biobased materials [10]. This effort makes the addition of biobased fillers in engineering thermoplastics attractive for applications such as under-the-hood shrouds. The incorporation of biobased fillers into the most consumed plastics can truly help offset the use of petroleum, while maintaining the mechanical integrity of manufactured parts. Furthermore with the right pretreatment, the incorporation of biobased fillers into engineering thermoplastics, traditional higher cost materials, the price of final goods could be reduced.

2.1. Experimental Goals

- Identify a viable pretreatment method to remove constituents within natural fibers with low degradation points.
- Pretreat various natural fibers and melt compound with engineering thermoplastics.
- Evaluate the thermo-mechanical properties of the engineering thermoplastic based biocomposites.

2.2. Analytical Goals

- Compare pretreatment results to determine the efficiency of the pretreatment on the various biomass feedstocks.
- Compare the thermo-mechanical property results of the engineering thermoplastic based biocomposites to those of the neat matrices to determine the effectiveness of the pretreated fiber as reinforcement in engineering thermoplastics.

2.3. Intended Outcome

The purpose of this work was to develop a viable method of pretreating natural fibers to remove constituents having low degradation temperatures, such that it could withstand the elevated processing temperatures of engineering thermoplastics.

CHAPTER 3. MATERIALS AND PROCESSING

In this work the materials used were chosen due to current commercial usage and local supply. The polymers used are some of the most widely used materials in commercial production which provides a broad application base for the biocomposites produced throughout this work. Natural fibers were chosen based on the local agricultural waste streams available. One of the goals for this work was to produce a high melting temperature biocomposites using traditional production methods. In this section are the material specifications and processing procedures utilized throughout this work.

3.1. Polyamide

Due to their abundant usage in commercial applications, polyamide 6 (PA6) and polyamide 6,6 (PA66) were used for this work. Both PA6 and PA66 were obtained from PolyOne, Avon Lake, Ohio. Ultramid 8202 manufactured by BASF Corporation, a low viscosity general purpose homopolymer was chosen for the PA6. Ultramid 1000-11 NF 2001 manufactured by BASF Corporation, a general purpose homopolymer was chosen for the PA66. Table 3.1 shows the published material properties for the two polyamides. Both grades of polyamide have comparable material properties with the largest difference coming in the melt temperatures. Choosing two materials with similar mechanical properties will allow the effects of varying processing temperatures to show in the biocomposite testing results.

Table 3.1: Material Properties for the Two Polyamides Used in this Work

	Melting Temperature (°C)	Density (g/cm^3)	Elastic Modulus (GPa)	Tensile Strength (MPa)	Flexural Modulus (GPa)	Flexural Strength (MPa)	Impact Toughness (J/m)
PA6	464 – 545	1.13	2.7	79.0	2.8	108.0	58.0
PA66	536 - 581	1.14	3.0	83.0	2.9	117.0	53.0

3.2. Biomass

For this work two biomasses have been chosen based on the available agricultural waste streams in the Fargo, North Dakota area. As North Dakota is one of the leading growers of sunflowers in the country, there is a natural waste stream from commodity processors in the area processing the seeds of the sunflower into consumer goods. During commodity processing, the seeds of the sunflower are removed from the flower and roasted for human consumption, packaged for bird or pet feed, or the protective hull is removed so the seed can be processed into oil, butter, roasted for consumption, etc. The hulls or shells of the seeds removed during the commodity processing have very low nutritional value; hulls can be substituted at no more than 20% of the feed for livestock. As the demand of hulls for the purpose of livestock feed is low, the waste stream is abundant and inexpensive [26]. Figure 3.1 shows the sunflower hulls as received from Red River Commodities, Fargo, North Dakota.

The second biomass chosen for this work is flax shive. Flax shive, unlike the outer protective nature of the sunflower hull, comes from the central woody core of flax stalk. Figure 3.2 shows a scanning electron microscopy image of a flax stem. The arrows point to the cuticle or protective outer layer of the flax stem. The area labeled F is the bast fiber which makes up flax fiber, underneath this is the cellulosic woody core of the stem, labeled area C, where shive comes from. Flax shive is a byproduct of flax fiber production. Flax

straw left on the field after flax seeds are harvested goes through a decortication process to remove flax fiber. By-products of decortication are then passed through sieves to remove any short fibers or seeds remaining and to sort out the various sizes of shive. The larger shive fractions are typically used as bedding for horses and the smaller fractions are used for biofuels and composite manufacturing. The flax shive used in this work was obtained from Flax Stalk Natural Fiber Solutions a subsidiary of Schweitzer-Mauduit International, Winkler, Manitoba, Canada. The as received flax shive can be seen in Figure 3.3.

Wet chemical analysis was performed by the Animal Sciences Department at North Dakota State University to determine the constituent makeup of the sunflower hulls and flax shive. AOAC standard 930.15 was used in dry matter determination, AOAC standard 920.39 was used to determine crude fat, and AOAC standard 2001.11 was used for the determination of crude protein. The USDA Agricultural Handbook No. 379 was followed for the analysis of neutral detergent fiber, acid detergent fiber, and acid detergent lignin. The constituent breakdown of the fibers used in this work can be seen in Table 3.2.

Figure 3.1: Sunflower hulls as received from commodity processors (right) and ground.

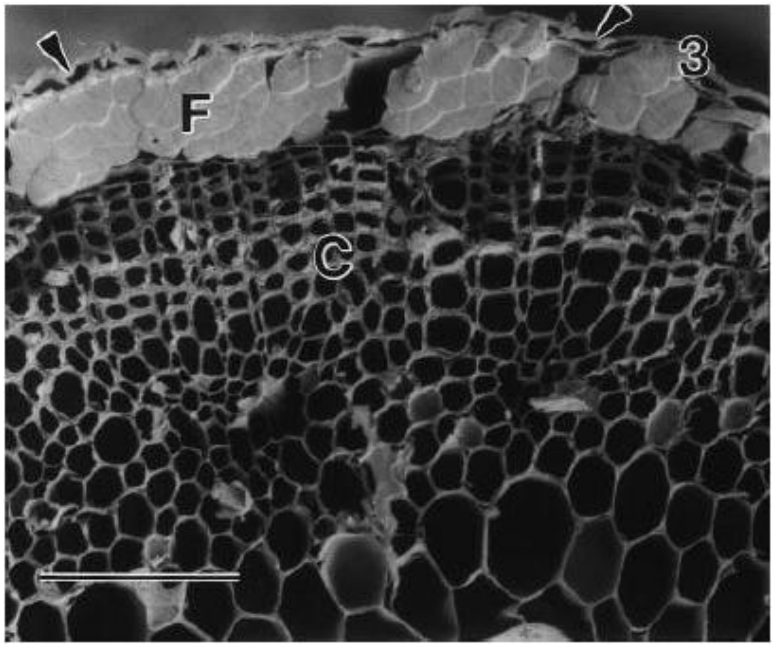

Figure 3.2: SEM image of a flax stem [27].


Figure 3.3: Flax shive as received from commodity processors.

Table 3.2: Constituent Breakdown for the Biomasses Used in this Study, All Numbers Are Weight Percentage.

Biomass	Lignin	Cellulose	Hemi-cellulose	Moisture	Ash	Starch	Calcium	Phosphorus	Crude Fat	Crude Protein
Sunflower Hull	22.4	39.8	15.1	7.1	2.7	0.6	0.3	0.17	7.0	5.3
Flax Shive	21.1	40.2	16.8	5.2	2.8	0.7	0.2	0.01	0.3	2.3

3.3. Torrefaction

As-received biomass was torrefied using a Lucifer model 7021-GT-E high temperature convection furnace. The chamber size for this furnace was 0.25 m wide, 0.27 m tall, and 0.51 m deep. The size of the chamber limited the amount of biomass that could be torrefied at one time. To prevent combustion of the biomass during the heating process an inert atmosphere was maintained using argon gas at a flow rate of approximately 5 psi/min. The biomass was heated to 300 °C and held at temperature for 8 hours. After the 8 hour torrefaction time the biomass was allowed to cool to room temperature while the inert atmosphere was maintained. After the torrefaction process, the torrefied flax shive (TFS) and sunflower hulls (TSFH) were stored in air tight containers until biocomposite processing was conducted. No fractionation of the TFS was done prior to biocomposite production. TSFH were fractionated using a blender prior to biocomposite processing. Figure 3.4 shows an example of biomass before and after the torrefaction process. Samples of the torrefied biomass were analyzed for moisture content prior to composite processing, moisture was undetected.

3.4. Twin Screw Extrusion

The biocomposites for this work were compounded using a Leistritz Micro-18/GL-40D, co-rotating twin-screw extruder. All torrefied fillers and polymer matrices were dried overnight at 80 °C in a convection oven. The polymer matrices, PA6 and PA66, were first dry blended with the torrefied biomass, TFS and TSFH, based on weight percentage. Three varying weight percentages were used for each biomass, 10 wt%, 20 wt%, and 30wt%. A temperature profile of: 193, 210, 216, 227, 238, 232, 227 °C starting at the feeding zone

and ending with the metering zone was used for PA6. For PA66 a temperature profile of: 236, 252, 258, 269, 280, 274, 269, 269 °C was used. The extruded biocomposites were water cooled, pelletized, and dried overnight at 80 °C in a convention oven prior to storing for injection molding.

Figure 3.4: The differences between torrefied biomass (left) and untorrefied biomass.

3.5. Injection Molding

The pelletized biocomposites were dried at 80 °C overnight in a convection oven prior to injection molding. A Technoplas, Inc. Model Sim-5080 injection molder was used for injection molding. The Technoplas molder has a single screw with four heating zones plus the injection nozzle. Temperatures for these zones from feeding zone to nozzle were: 260, 271, 277, 277, 277 °C was used for PA6. For PA66 a temperature profile of: 271, 282, 293, 299, 304 °C was used. Geometries of the final specimens were dog bones and rectangular bars approximately 3.2 mm thick.

3.6. Specimen Preparation

As stated in American Society of Testing and Materials (ASTM) testing standards the injection molded specimens were conditioned prior to mechanical testing. The specimens were placed in a Boekel dricycler for a minimum of 48 hours before testing was conducted. The specimens were then stored in the dricycler until all specimens were tested to ensure proper conditioned moisture content and temperature.

CHAPTER 4. EXPERIMENTAL PROCEDURES

The ultimate goal of this work is to produce a polyamide biocomposite which exhibits improved mechanical properties to those of the base polymer. To evaluate the effectiveness of the torrefied filler in the polyamide matrix, a full mechanical and thermo-mechanical analysis was performed. This section describes all the procedures used to evaluate the biocomposites as well as the neat matrix. Unless otherwise noted, all testing was conducted at room temperature under laboratory standards.

4.1. Tensile Modulus and Strength

Tensile modulus and strength were evaluated according to ASTM standard D638, standard test method for tensile properties of plastics. An Instron Model 5567 load frame equipped with a 30 kN load cell was used for all tensile testing. An MTS model 632.35B-200 extensometer was used to record strain during the first portion of the testing. Once the specimen reached 20% elongation, the test was paused while the extensometer was removed. Testing then continued until failure occurred or the load peaked and necking began. For each grade of material, five specimens were tested at a cross head rate of 5 mm/min. Tensile modulus was calculated using the extensometer readings and tensile strength was recorded as the maximum stress achieved.

4.2. Flexural Modulus and Strength

Flexural modulus and strength were determined according to ASTM standard D790, standard test methods for flexural properties of unreinforced and reinforced plastics and electrical insulating materials. The Instron load frame described above was also used for all

flexural testing. For each grade of material, five specimens were tested using 3.2 mm diameter loading and support pins. Flexural strength was recorded as the maximum stress achieved and flexural modulus was calculated from extension readings.

4.3. Impact Toughness

ASTM standard D256, standard test methods for determining the Izod pendulum impact resistance of plastics, was used to evaluate the impact toughness of the biocomposites. A pendulum weight of 4.497 N was used, following procedure A . Each specimen was notched with a 2.54 mm notch prior to testing using a Veekay Testlab Veekay Notch Cutter. A total of six specimens were tested for each grade of material. Impact toughness was calculated using the energy absorbed by the specimen and the area at the notch region. In accordance with the ASTM standard any specimen with a crack propagation less than 90% of the width of the specimen were considered a non-failure.

4.4. Immersion Density

The densities of the materials being studied were determined using a Mettler Toledo 33360 immersion density kit. All testing was conducted at room temperature in isopropyl alcohol to avoid any uptake of liquid during the testing. The density for each specimen (ρ) was calculated using the following equation:

$$\rho = \frac{m_{dry}}{m_{dry} - m_{immersed}} * \rho_{fluid}$$

where m_{dry} is the dry mass of the specimen prior to immersion, $m_{immersed}$ is the mass of the specimen when immersed in the fluid, and ρ_{fluid} is the density of the fluid. Six specimens were used to determine the density of each grade of material.

4.5. Moisture Uptake

An Arizona Instruments Computrac 4000XL Moisture Analyzer was used to determine the moisture uptake of the materials. Specimens were soaked in distilled water for 24, 72, and 168 hour intervals. Adsorbed moisture was removed by towel drying the specimens prior to analysis. Each specimen was heated to 210 °C and while maintaining this temperature, mass loss was recorded. Once the mass loss slowed to 0.015% moisture/minute, the analysis was complete and the total mass loss measured was recorded as the total moisture absorbed. A total of three specimens were analyzed for each material grade at each soak length. To reduce the error from retesting specimens, a new specimen was used for each test.

4.6. Dynamic Mechanical Analysis

A TA Instruments Q-800 Dynamic Mechanical Analyzer (DMA) was used to determine the glass transition temperature of the materials. These tests were conducted according to ASTM standard D7028, standard test method for glass transition temperature of polymer matrix composites by dynamic mechanical analysis. Using a dual cantilever fixture, specimens were subjected to an amplitude of 20 μm at a frequency of 20 Hz while the temperature was raised at 3 °C/min up to 200 °C. The glass transition temperature was taken as the temperature at the peak of the tangent delta curve. Storage modulus was also studied. Figure 4.1 shows an example curve used to determine the glass transition temperature and storage modulus. A total of four specimens were tested for each material grade.

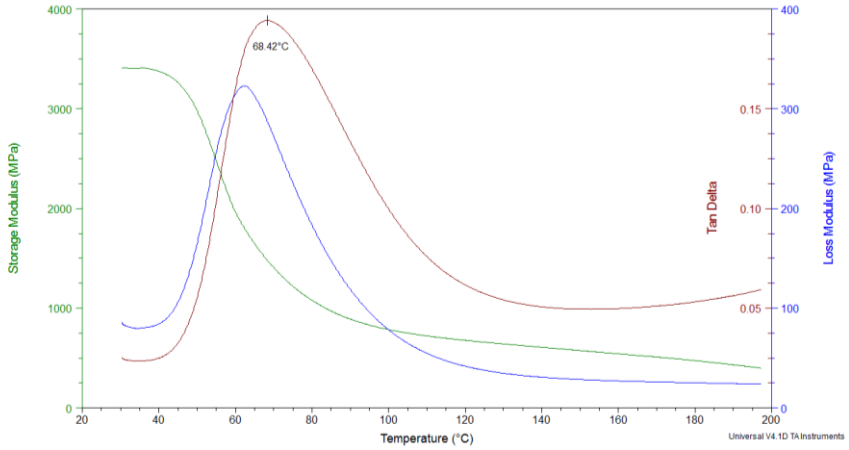

Figure 4.1: Example of a graph used to determine glass transition temperature.

4.7. Heat Deflection Temperature

A modified ASTM standard D648, standard test method for deflection temperature of plastics under flexural load in the edgewise position, was used to determine the heat deflection temperature of the materials. The ASTM standard was modified to use the TA Q-800 DMA with a three-point bending fixture installed. Specimens were subjected to a constant stress of 0.455 MPa while the temperature was increased at 3 °C/min up to 200 °C. Due to the limit specimen size using the DMA, the specified deflection in D648 was converted to a strain based on the standard dimensions. This strain of 0.121 % was then used to determine at what deflection in the smaller DMA samples the standard strain was achieved. The temperature at which the determined deflection occurred was taken as the heat deflection temperature. A total of four specimens were tested for each material grade.

4.8. Coefficient of Linear Thermal Expansion

ASTM standard E831, standard test method for linear thermal expansion of solid materials by thermomechanical analysis, was used as a guide to determine the linear

thermal expansion of the materials. Using the above described DMA equipped with a film tension fixture, specimens were heated at 5 °C/min up to 200 °C. Using a strain versus temperature plot the slope of the linear region prior to the glass transition temperature is recorded as the coefficient of linear thermal expansion. Figure 4.2 shows an example of the strain versus temperature graph. A total of four specimens were tested for each material grade.

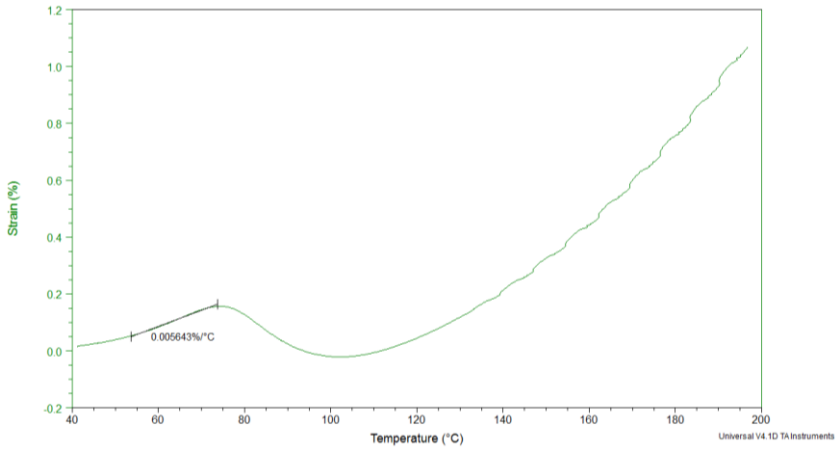

Figure 4.2: Example of a graph used to determine coefficient of linear thermal expansion.

4.9. Melt Flow Index

According to ASTM standard D1238, standard test method for melt flow rates of thermoplastics by extrusion plastometer, melt flow index (MFI) was measured for the materials. A Tinius Olsen Model MP600 melt flow indexer with a 225 g mass was used for this testing. Procedure A with a travel distance of 2.25 cm and a set temperature of 270 °C was used to capture the MFI. For each grade of material one sample was measured.

4.10. Microscopy

Optical microscopy was used to analyze the void content of the molded specimens. Small specimens of the material were cast in vinyl ester and polished prior to microscopy with sandpaper. Images taken with a Zeiss Axiovert 40 MAT microscope equipped with a ProgRes C10 camera were used to evaluate void content. Figure 4.3 shows an example image used to determine the void content.

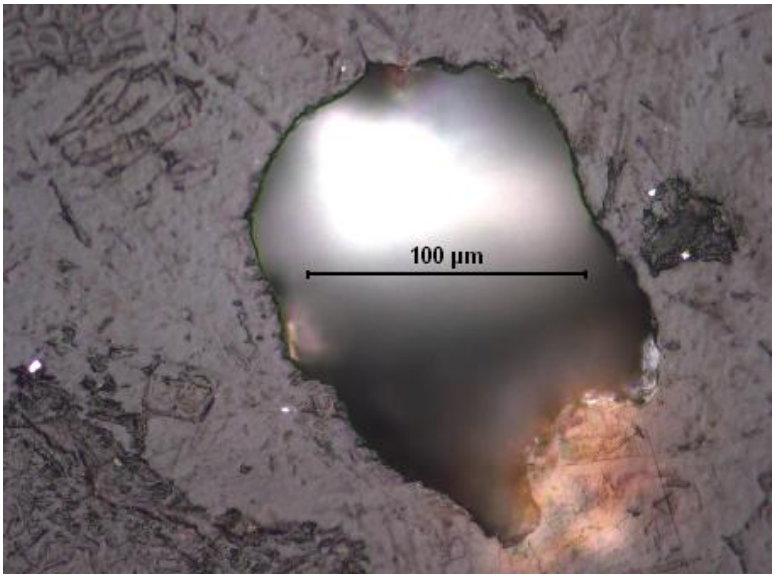

Figure 4.3: Example image used to determine void content in polyamide biocomposites.

CHAPTER 5. RESULTS AND DISCUSSION

5.1. Processing and Proof of Concept

To ensure uniform effects from the processing parameters among all the grades of materials, an attempt at extruding the neat polyamide was made. However, a low melt viscosity made it very difficult to extrude a continuous strand and the strands that were produced had diameters of < 1 mm. The temperature profile for the neat polymer also had to be quite high (~300 °C) to prevent the polymer stream from freezing off at the die of the extruder. With the addition of torrefied biomass, the melt viscosity increased, improving the extrusion process. The addition of torrefied biomass blocked the movement of the polymer chains resulting in an increased melt viscosity. The addition of torrefied biomass also allowed the temperature profile to be decreased to the low end of the melting zone for polyamides. This decrease in melting temperature can be explained by a decrease in molecular weight when torrefied biomass is added to the polyamide matrix, this will be shown later through the investigation of melt flow index.

The initial step for this work was to show the effectiveness of torrefaction in preparing the biomass for introduction into engineering thermoplastic matrices, whose processing temperatures exceed the degradation temperature of natural fibers. Two biocomposites were extruded and molded for testing, one using untreated sunflower hulls and the other using TSFH. Figure 5.1 shows the results of tensile testing for these two biocomposites. It can be seen from Figure 5.1 that the torrefaction leads to improved tensile performance over the untreated sunflower hulls. Also of note is the difference in variations. The TSFH filled biocomposites displayed lower variations than the untreated sunflower hulls. Table

5.1 shows the coefficients of variation computed for both the tensile strength and elastic modulus data; the untorrefied sunflowers hull biocomposites had coefficients of variation more than twice that of the TSFH biocomposites. During processing of the TSFH biocomposites the melt strength was observed to increase. There were noticeable differences in odor and off-gassing during processing too; the untorrefied filler had the distinct odor of burning biomass, while the torrefied filler displayed no noticeable odor.

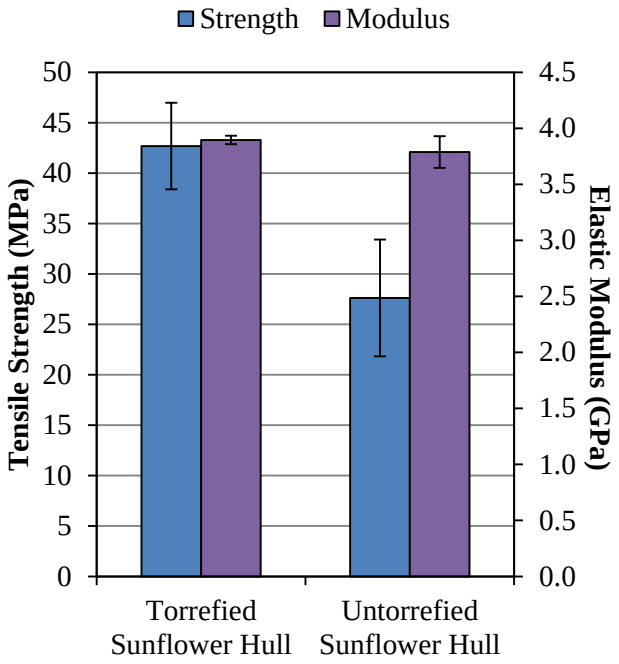

Figure 5.1: Tensile property results for torrefied and untorrefied sunflower hulls.

Table 5.1: Coefficients of Variation for Torrefied and Untorrefied Sunflower Hull Biocomposites

	Tensile Strength Coefficient of Variation (%)	Elastic Modulus Coefficient of Variation (%)
Torrefied Sunflower Hulls	10.05	0.98
Untorrefied Sunflower Hulls	20.95	3.73

Both PA6 and PA66 biocomposites were compounded for this study. During the injection molding process the PA66 biocomposites off-gassed. As the PA6 biocomposites

molded without any issues, it is believed this off-gassing is due to further degradation of the biomass fillers. Although the torrefaction was done at 300 °C the molding temperatures of PA66 are right around 300 °C, if the torrefaction of biomass was not completely successful further degradation could have taken place. If this was the case, it did not happen with the PA6 biocomposites because of the lower processing temperature, 277 °C. Several attempts were made to mold specimens but the polyamide biocomposites were too void ridden and did not survive the de-molding process. Figure 5.2 shows examples of the voids observed in the PA66 biocomposites.

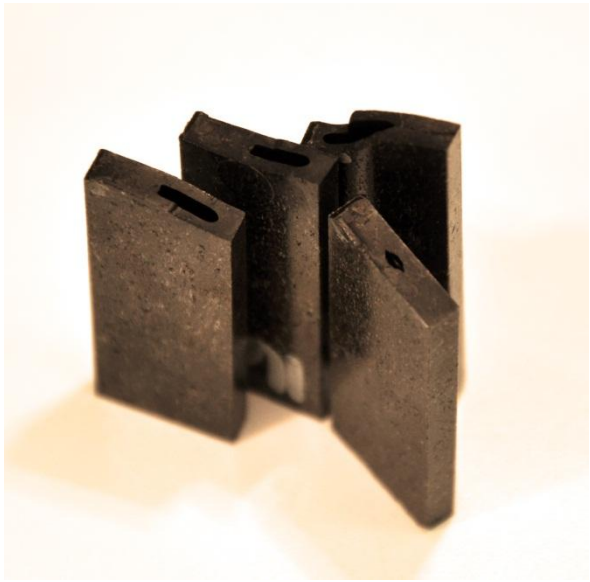

Figure 5.2: Voids observed in PA66 biocomposites.

5.2. Torrefaction

With the initial proof of concept experiment showing promising results for reinforcing high temperature thermoplastic biocomposites, larger batches of torrefied fillers were produced. Sunflower hulls were expected to have a yield of 62.6%, the total mass content of the dry untreated hulls accredited to cellulose and lignin as shown in Table 3.2. For flax

shive the yield was expected to be 61.3%. Figure 5.3 shows the sunflower hulls prior to and after the torrefaction process has taken place. The color of the TSFH is of note, the darker fibers are indicative of a full torrefaction, however the lighter brown fibers indicate a milder torrefaction. Figure 5.4 shows the difference in untreated flax shive and TFS. With the variation in colors it was concluded that the lab scale torrefaction used in this work was not a uniform and complete process. This is due to the equipment available; a more uniform consistent process would be needed to validate the use of torrefied biomass on a commercial scale.

Figure 5.3: The difference between untreated sunflower hulls (left) and torrefied sunflower hulls (right).

Figure 5.5 and Figure 5.6 show the FTIR results for the TFS and TSFH in comparison with the untreated biomass. FTIR indicated that for TFS the carbon-carbon double bond absorbance intensity increased, indicating the presence of more bonds in the TFS. The increase in carbon-carbon double bonds in indicative of the conversion of the constituents within lingo-cellulosic materials to carbon. The decreases observed in the intensity of the peaks between 3000-3600 cm^{-1} for both TFS and TSFH indicates the dehydration of

cellulose and lignin content. While the curves between the torrefied biomasses showed similar intensities, it is interesting that between the untreated sunflower hull and flax shive the FTIR intensities are rather different. Over all the sunflower hull produced higher intensities than the flax shive. For the TSFH the changes observed in peak intensity between 650 cm^{-1} and 1650 cm^{-1}indicates that torrefaction is changing the chemical structure of the biomass. The TFS FTIR depicts a very different scenario; the lack of change in the peaks, beyond lower intensities, indicates the torrefaction was not complete. Some further investigation is need to truly understand how the torrefaction processed used in this work has changed the biomass.

Figure 5.4: The difference between untreated flax shive (left) and torrefied flax shive (right).

The small lab scale process employed in this work limited the size of a single torrefaction batch to approximately 200 g of untreated biomass to begin with, that only yields approximately 120 g of torrefied biomass. For this reason the torrefaction for all the biocomposite grades was done prior to any composite processing so the multiple batches

needed, could be mixed together. This helped ensure that any differences among torrefaction batches did not affect the mechanical performance of the biocomposites.

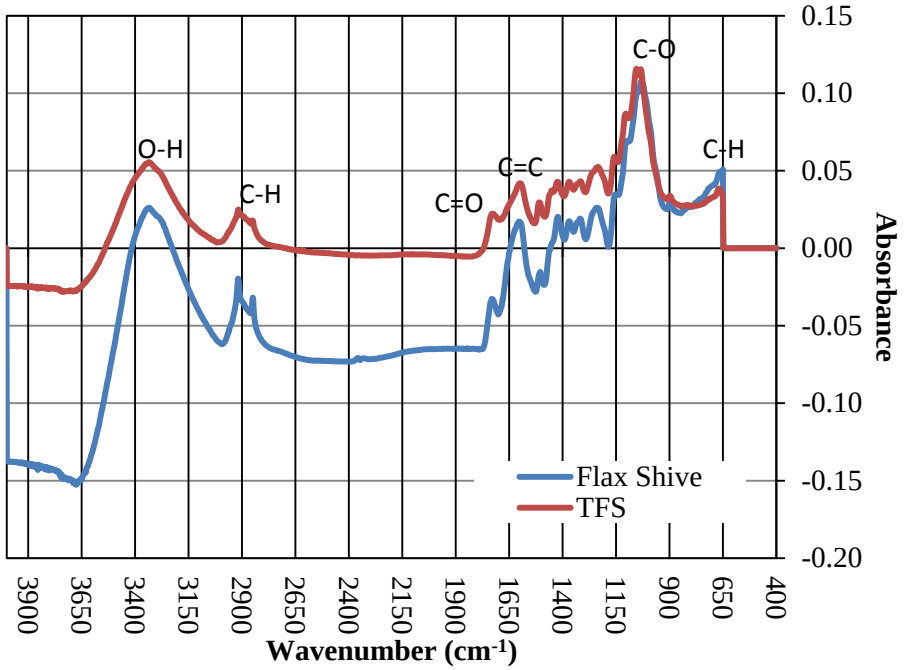

Figure 5.5: FTIR of TFS and untreated flax shive.

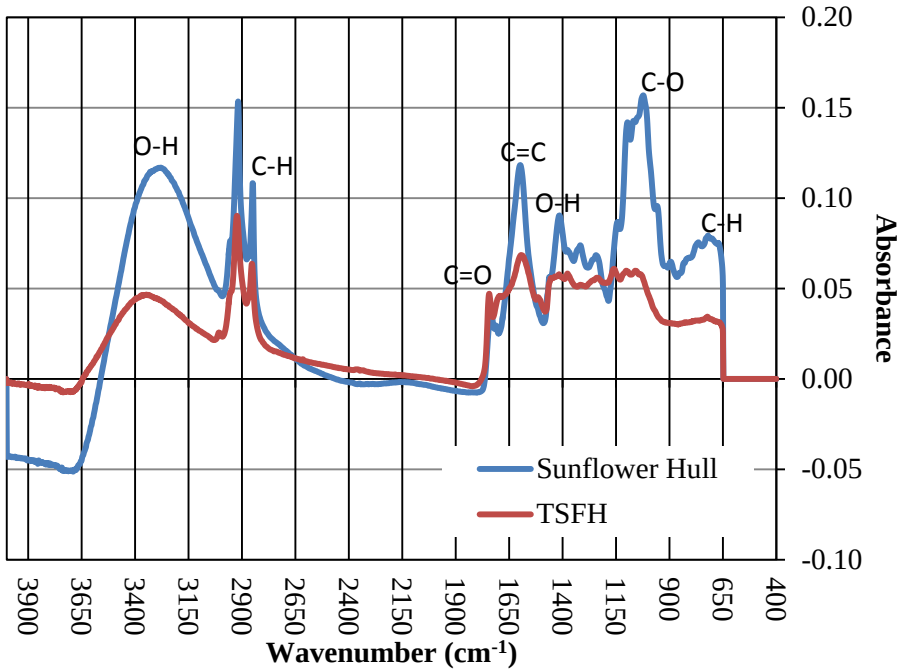

Figure 5.6: FTIR of TSFH and untreated sunflower hull.

5.3. Tensile Modulus and Strength

Figure 5.7 and Figure 5.8 show the tensile property results of the PA6 biocomposites utilizing TFS and TSFH respectively. For both the TFS and the TSFH, the tensile strength saw minor decreases from that of the neat polymer. The TFS showed a very slight decrease in tensile strength with increased filler loading, while the TSFH biocomposites a slight increase in strength at the 20 wt% loading. From the literature reviewed, it was expected to see slight increases to the strength from the matched polarities of the biomass and matrix. However, as discussed prior, the torrefaction used in this work was not a complete and uniform process. It is possible that the filler is still undergoing some degradation during processing, hindering the fiber-matrix bond. It is a possibility that void content within the specimens may have played a role as well. This will be discussed later.

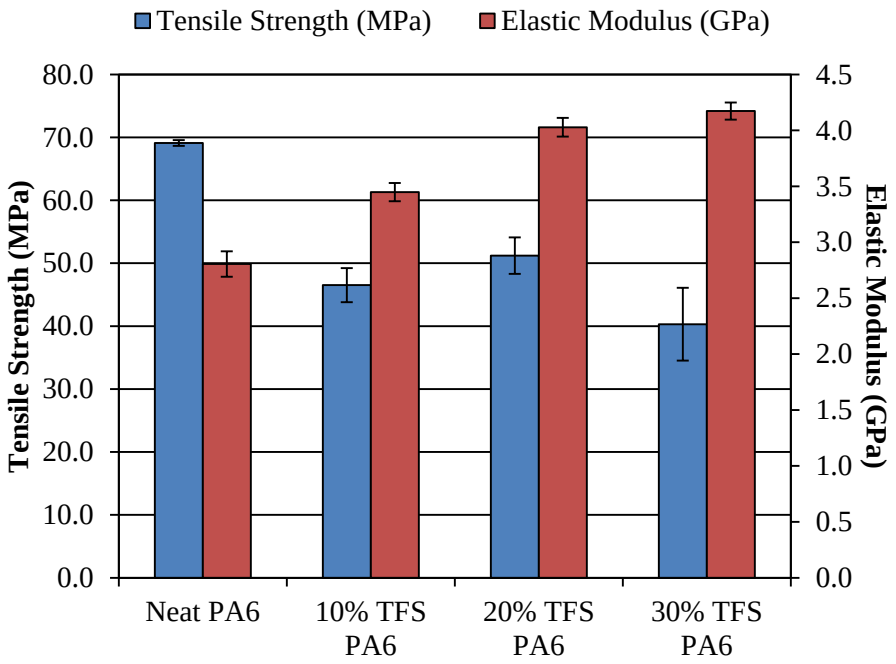

Figure 5.7: Tensile properties for torrefied flax shive reinforced PA6.

As would be expected with the addition of fillers to a polymer matrix, the elastic modulus increased with increased filler loading. When filler is introduced into a polymer matrix of similar polarity, the fibers begin making hydrogen bonds with the matrix. These hydrogen bonds along with the addition of stiffer filler, chain movement is restricted within the material thus increasing stiffness and elastic modulus. TFS and TSFH both displayed similar tensile properties. TSFH displayed slightly higher tensile strengths than TFS at higher filler loadings while TFS displayed slightly higher elastic moduli than TSFH. However, neither TFS or TSFH showed to be significantly better than the other.

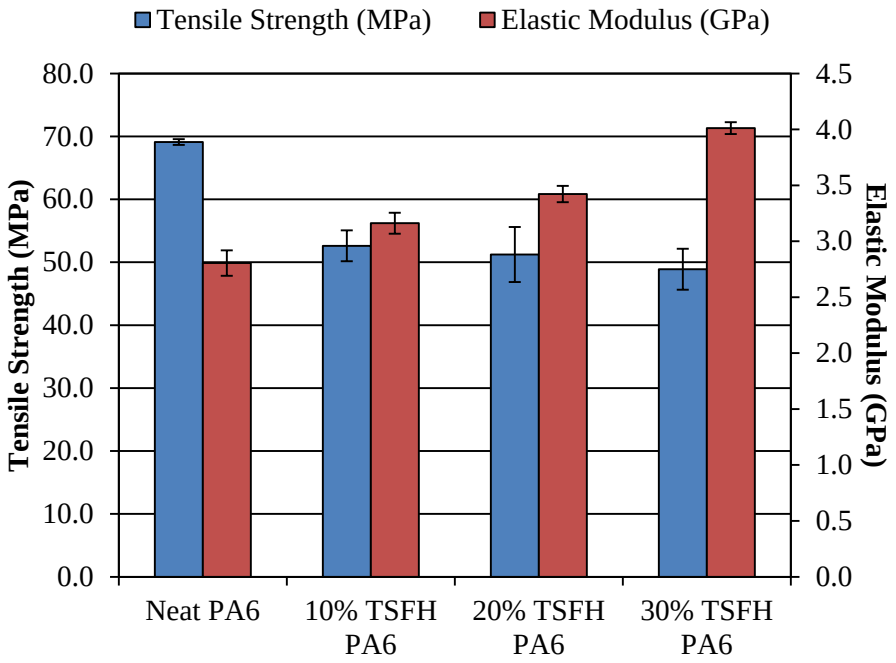

Figure 5.8: Tensile properties for torrefied sunflower hull reinforced PA6.

5.4. Flexural Modulus and Strength

Flexural strength and modulus results can be seen in Figure 5.9 and Figure 5.10 for TFS and TSFH filled PA6. As would be expected when adding fillers to polymer matrices, the flexural properties increase. For the TFS filled biocomposites, the flexural strength

showed a minor decrease as compared to the neat matrix, but there was a steady increasing trend with increased filler loading. This slight decrease could be due to thinner fibers that buckle under flexural stress. The TSFH showed an increase over the neat matrix but with added filler there was no significant change in the strength. For both the TFS and TSFH, tangent modulus exhibited an increasing trend with increased filler loading. TSFH displayed higher flexural strengths than the TFS; this may be due to the larger filler sizes going into the extrusion process.

5.5. Impact Toughness

Impact toughness for TFS and TSFH PA6 biocomposites can be seen in Figure 5.11 and Figure 5.12, respectively. Both the TFS and TSFH fillers showed decreasing trends in impact toughness with increased filler loading. The bond between fiber and matrix restrict the polymer chain movement, transferring the applied loads from matrix to fiber. While these interactions are beneficial to increasing both elastic and tangent moduli, they hinder the ability of the biocomposite to absorb energy during impact events. Although there is decease observed with increased filler loading, the drop is not as detrimental as that seen in polyolefin biocomposites[28], this is likely due to the improved fiber-matrix bond of the hydrophilic polyamide and torrefied biomass. No clear differences are present between the impact toughness of TFS and TSFH reinforced PA6.

5.6. Density

Torrefaction is a densification process, meaning the biomass going into the process is much less dense than the torrefied biomass. This then leads to the expectation that the

torrefied biomass filled biocomposites will have increasing densities with increasing filler loadings. Figure 5.13 and Figure 5.14 show the densities of the TFS and TSFH biocomposites studied in this work, respectively. In Figure 5.13 at 10 and 20 wt% loading the densities increased over the neat matrix as would be expected. At 20 wt% loading however, the variation was quite high, indicative of voids in the specimens or irregularities among specimens. When the filler loading was increased to 30 wt% loading, the density dropped below the neat polyamide. Again this is likely due to voids within the specimens. Microscopy was used to evaluate the void content and will be discussed later. Figure 5.14 shows the TSFH biocomposites displayed an increasing trend with increasing filler loading. At the 20 wt% and 30 wt% loadings the densities did increase but the variation was larger than the neat matrix and 10 wt% loading. This could again be due to voids within the specimens. No clear difference between the densities of TFS and TSFH biocomposites were observed.

5.7. Moisture Uptake

Polyamide materials are known for absorbing moisture form the environment. While the moisture saturation point is around 8% and equilibrium moisture content is approximately 2%, the addition of torrefied biomass has the potential to reduce moisture uptake during end use of the material. The biggest concern with the uptake of moisture for polyamides is the degradation of mechanical performance as the amount of moisture in the material increases [13].

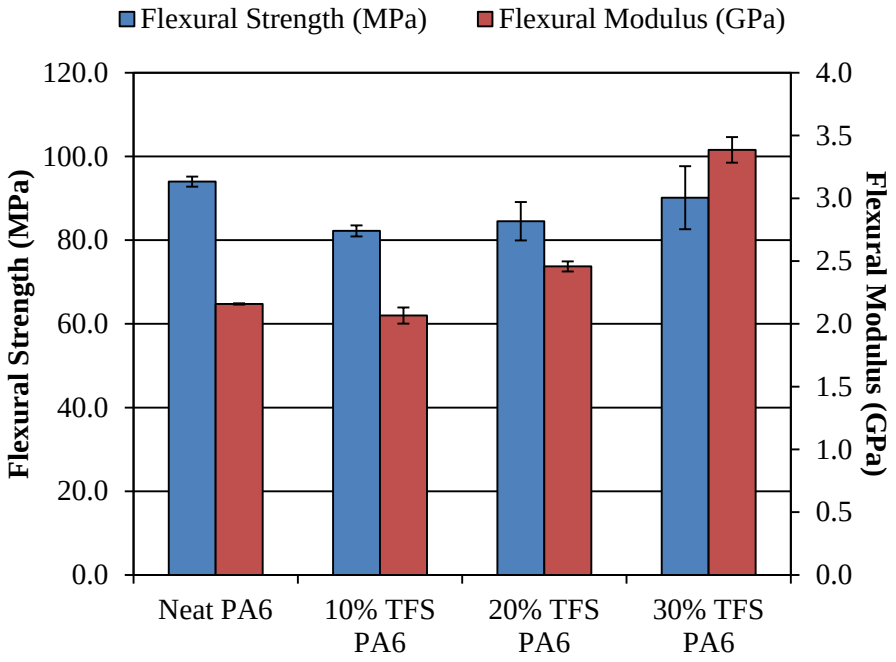

Figure 5.9: Flexural properties for torrefied flax shive reinforced PA6.

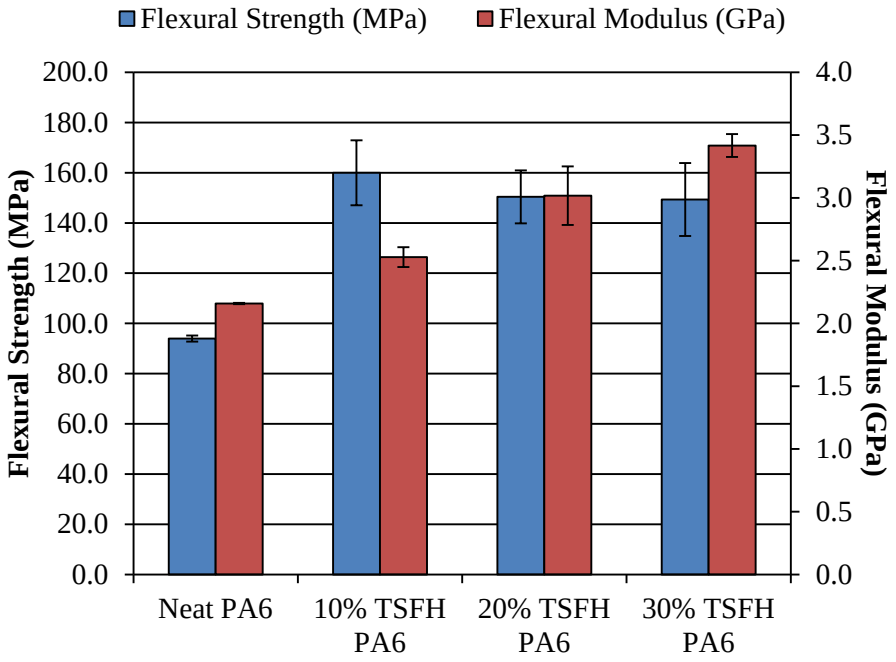

Figure 5.10: Flexural properties for torrefied sunflower hull reinforced PA6.

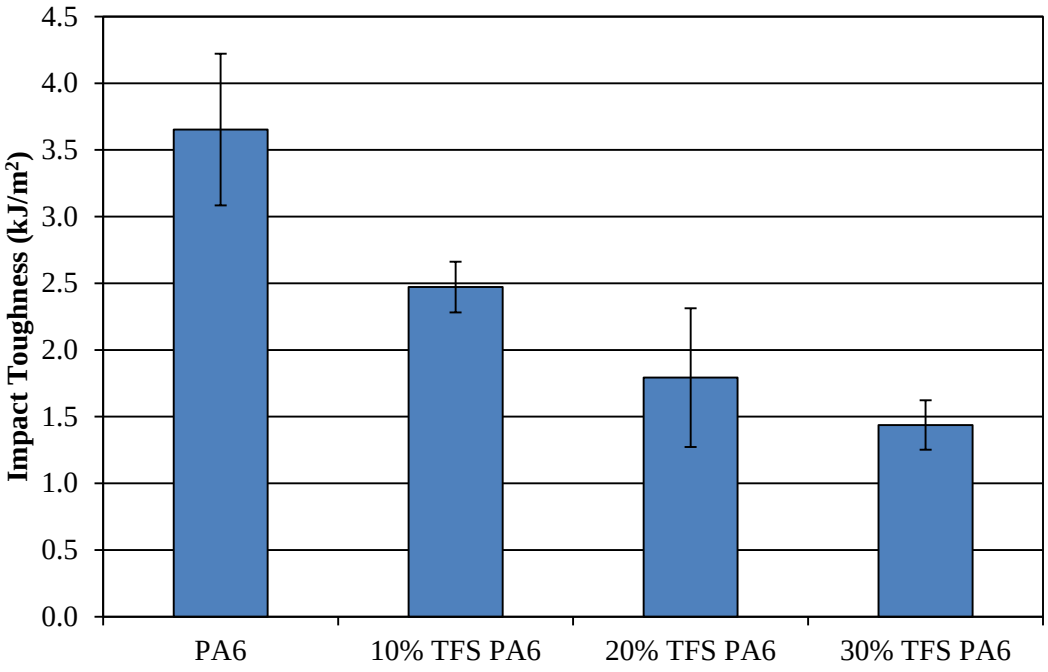

Figure 5.11: Impact toughness of torrefied flax shive reinforced PA6.

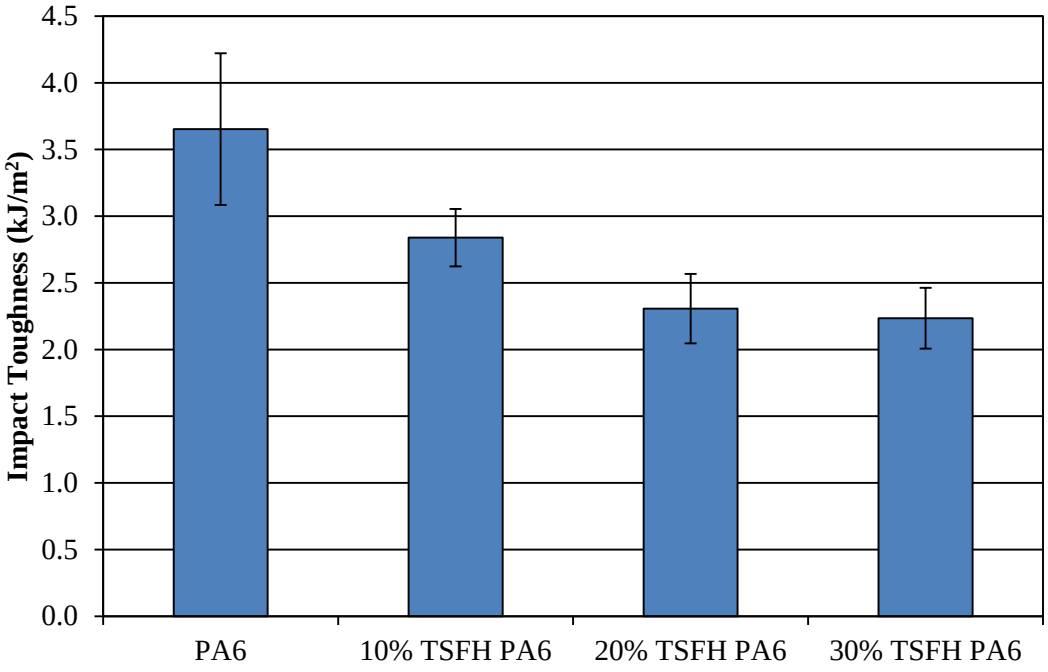

Figure 5.12: Impact toughness of torrefied sunflower hull reinforced PA6.

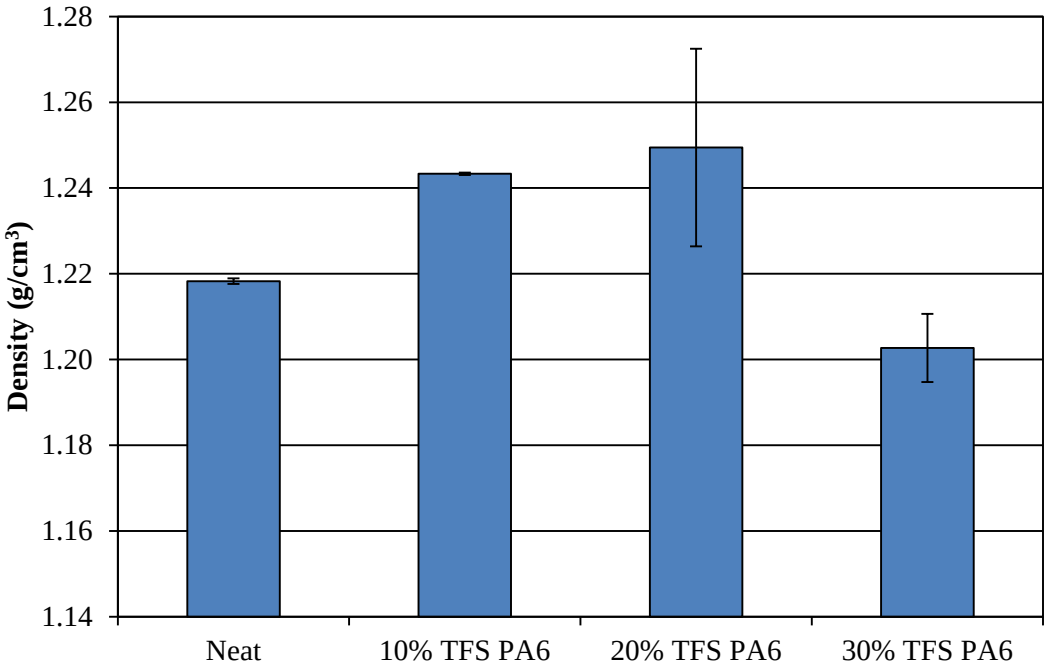

Figure 5.13: Density of torrefied flax shive reinforced PA6.

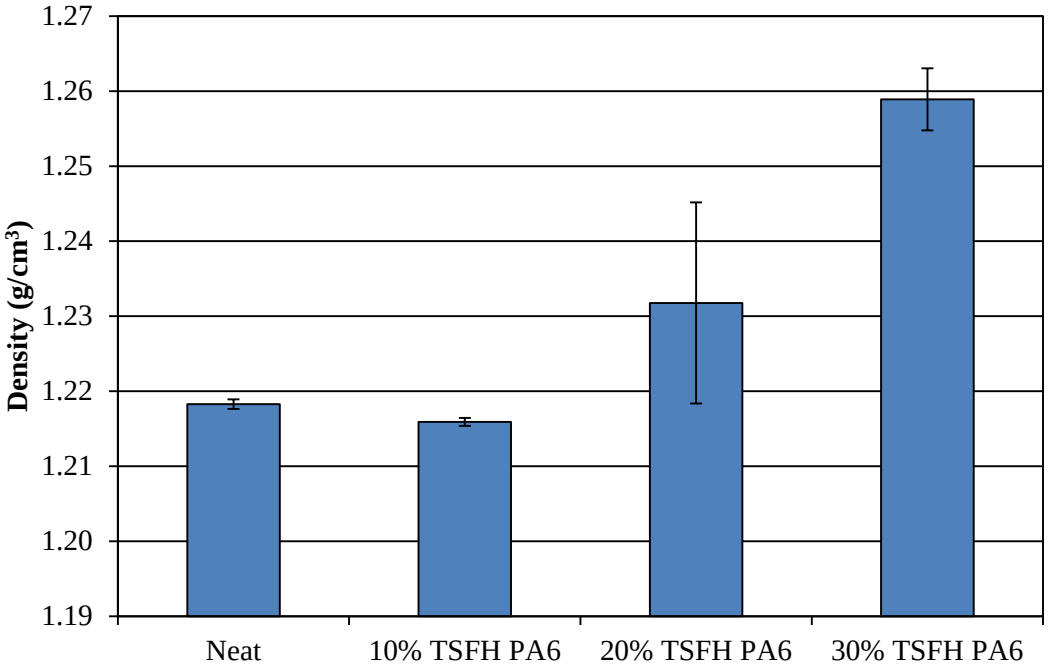

Figure 5.14: Density of torrefied sunflower hull reinforced PA6.

Figure 5.15 shows the moisture uptake of TFS PA6 biocomposites at 24, 72, and 168 hours soaks. At 24 hours the biocomposites did take on less moisture than the neat matrix.

At 72 hours the biocomposites absorb less moisture than the neat matrix but the difference is not as significant as it was at 24 hours. At 168 hours the biocomposites absorb more moisture than the neat matrix. However, at the lower filler loadings the moisture absorption was lower than it was at 72 hours. To ensure the thermal effects of the moisture analysis did not play a role in the results, new specimens were used for every test in the moisture study. The presence of voids which will be discussed further could be playing a role in the phenomenon. Another explanation could be that the torrefied filler retards the rate at which moisture is absorbed until the material beings to become saturated. Full saturation was not reached in this study but some future work could shed some light on what is really happening with the TFS biocomposites.

Figure 5.16 shows the moisture uptake results for the TSFH filled PA6 biocomposites. These materials displayed increasing trends with increasing soak times, which is to be expected. The more important trend to note is the decreased moisture uptake with the added filler. All the TSFH filled biocomposites displayed lower moisture uptake over the neat matrix. The higher filler loadings did display higher variations than the neat matrix. There are a number of explanations for the variation observed at higher filler loadings; voids within specimens filled with absorbed moisture increasing the ultimate moisture content, residuals oils on the fibers acted as a moisture absorption retardant, or the variation within the specimen sizes may have led to induced variation of the moisture absorbed. The TSFH biocomposites did display higher affinity to moisture at the 168 hour soak than the TFS biocomposites, however the questionable results for TFS may be the reason for this difference as the 24 and 72 hour results are very similar.

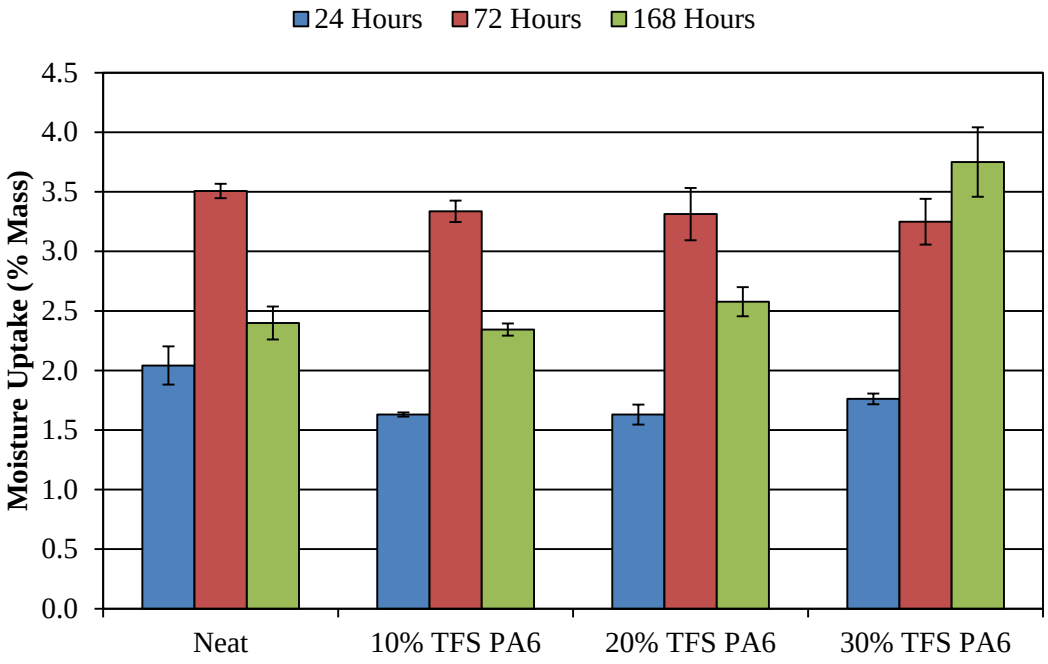

Figure 5.15: Moisture absorption of torrefied flax shive reinforced PA6.

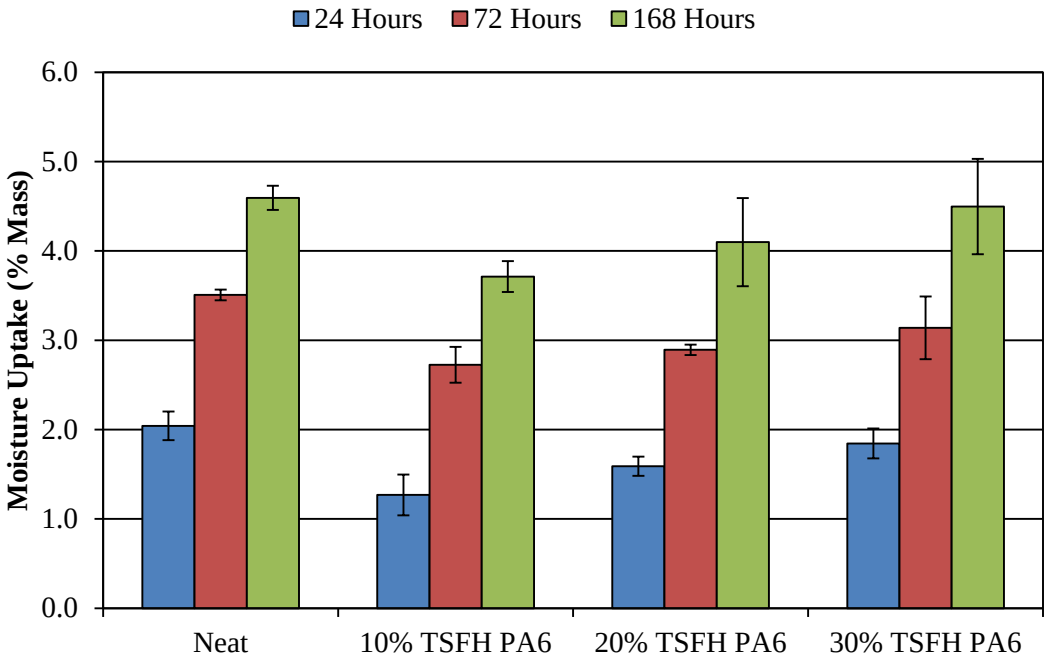

Figure 5.16: Moisture absorption of torrefied sunflower hull reinforced PA6.

5.8. Dynamic Mechanical Analysis

Much like the increasing trends observed in the elastic and tangent moduli, the dynamic mechanical properties should see similar trends. The molecular chains with in the polymer are restricted in movement due to the added filler; this also translates into restricted movement under elevated temperatures. Figure 5.17 and Figure 5.18 show the glass transition temperatures for the TFS and TSFH biocomposites respectively. The TSFH biocomposites show a slight decrease with the added torrefied biomass, 10 °C at the most. The TFS biocomposites show no significant change with added filler content. Table 5.2 and Table 5.3 show the ANOVA analysis of glass transition temperatures for the TFS and TSFH biocomposites respectively. TFS displayed high P-value thus indicating there is no significant influence of torrefied biomass content on the glass transition temperatures observed. The TSFH on the other hand displayed a very low P-value indicating the decrease observed with added filler content was significant. Between the TFS and TSFH biocomposites glass transition temperatures remained very close.

Table 5.2: ANOVA Analysis of TFS PA6 Biocomposites

Source	Degrees of Freedom	Sum of Squares	Mean Square Error	F	P
TFS Content	3	15.83	5.28	2.50	0.109
Error	12	25.34	2.11		
Total	15	41.17			

Table 5.3: ANOVA Analysis of TSFH PA6 Biocomposites

Source	Degrees of Freedom	Sum of Squares	Mean Square Error	F	P
TSFH Content	3	278.145	92.715	105.08	0.000
Error	12	10.587	0.882		
Total	15	288.733			

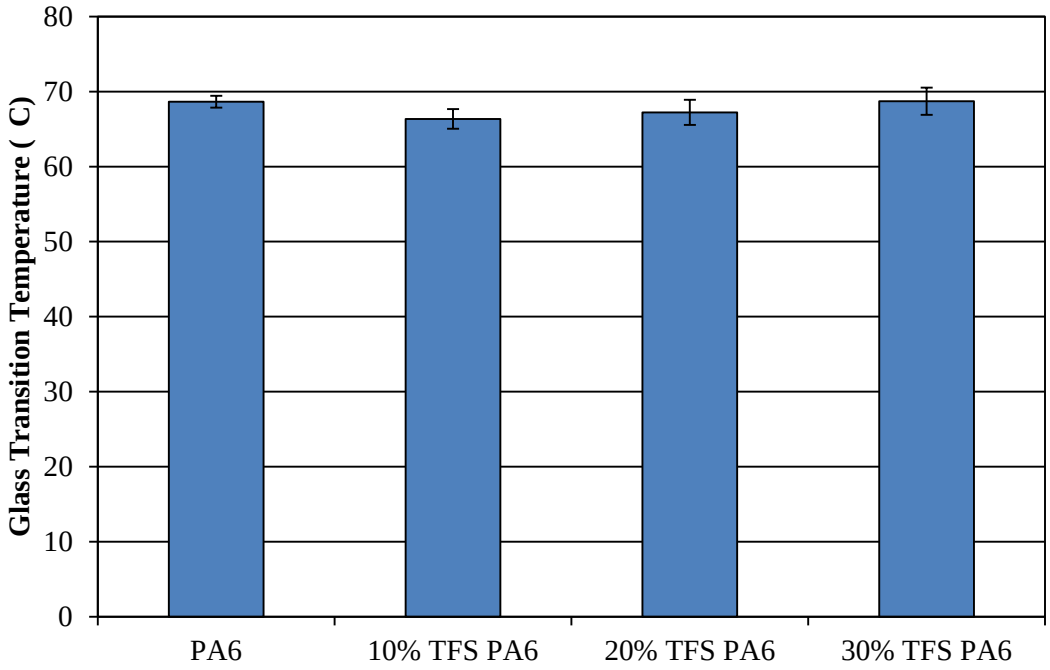

Figure 5.17: Glass transition temperature of torrefied flax shive reinforced PA6.

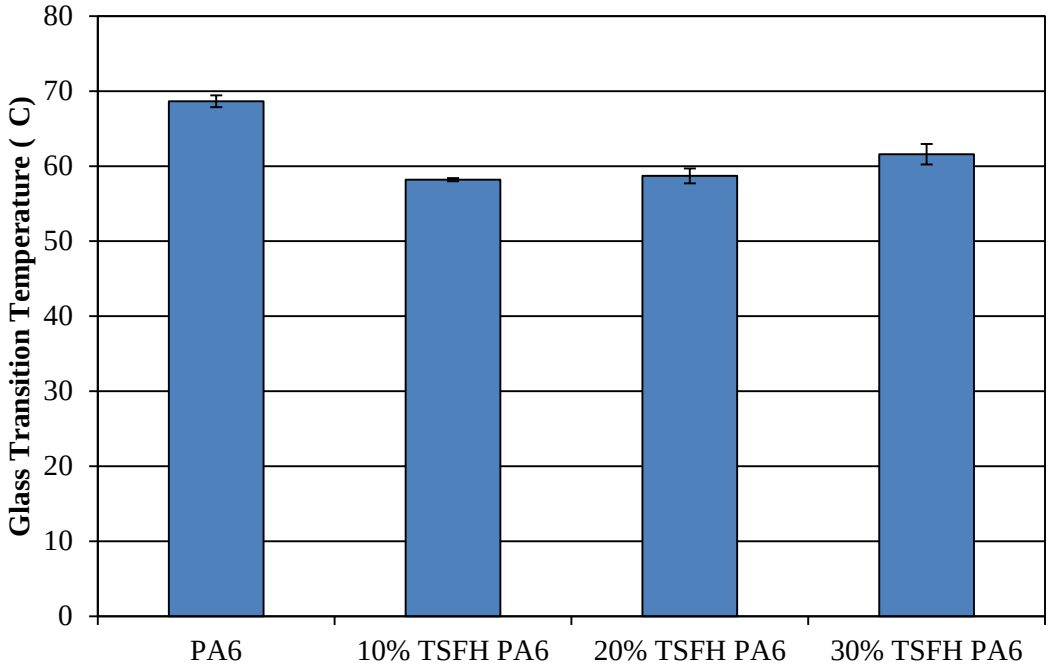

Figure 5.18: Glass transition temperature of torrefied sunflower hull reinforced PA6.

Figure 5.19 and Figure 5.20 show the storage moduli trends for TFS and TSFH biocomposites respectively. As was seen with the previously discussed moduli, the storage

modulus of the TFS displays an increasing trend with increased filler loading. The decreasing trend with increased temperature is to be expected as the polymer chains relax with increased temperature, as they slide past one another much easier. The addition of torrefied biomass also decreased the rate at which temperature effects storage modulus. As the temperature increased and polymer chains relaxed the filler remains rigid and impedes the chain movement of the polymer. The TSFH storage modulus results are interesting; all four of the TSFH moduli curves are very close together and approximately 1000 MPa lower than the TFS composites. There are no clear differences between the varying filler loadings like with the TFS composites. There is a decreasing trend with temperature, and the biocomposites are all higher than the neat matrix above the glass transition temperature. However, below the glass transition temperature the neat matrix has a higher modulus.

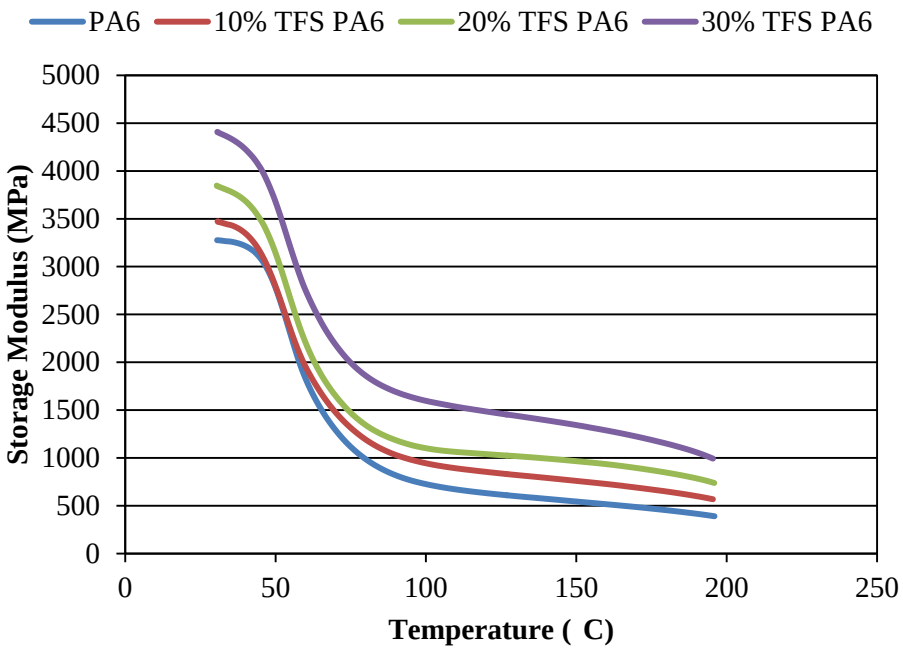

Figure 5.19: Storage modulus of torrefied flax shive reinforced PA6.

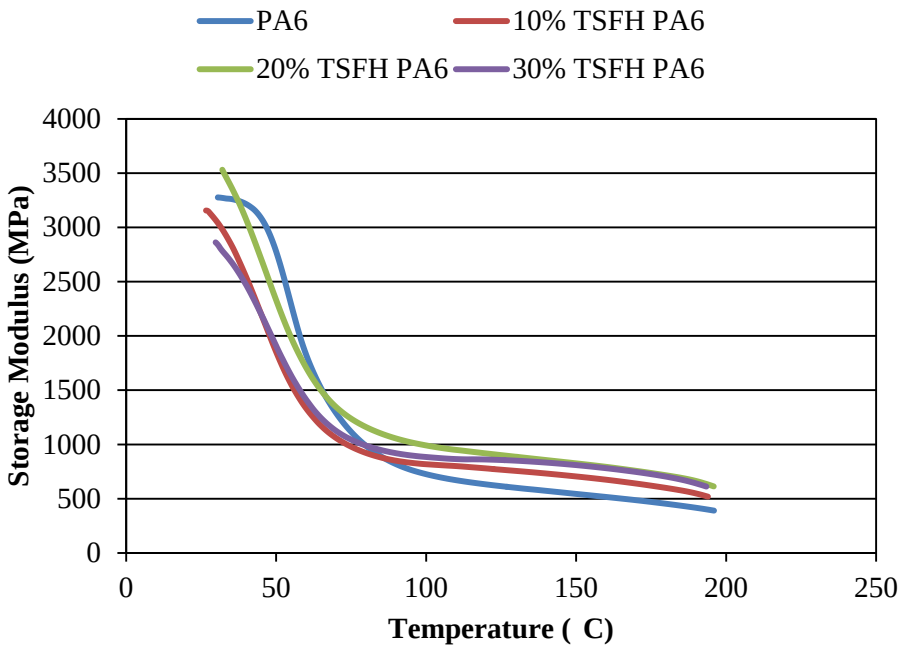

Figure 5.20: Storage modulus of torrefied sunflower hull reinforced PA6.

5.9. Heat Deflection Temperature

Much like the trends in tensile and flexural moduli, heat deflection temperature is also expected to increase with increased filler loadings. The increased stiffness of the biocomposites due to restricted polymer chain movement is maintained at elevated temperatures. Figure 5.21 and Figure 5.22 show the heat deflection temperatures measured from three-point bend testing using a dynamic mechanical analyzer. Both fillers showed positive trends with increasing filler loading. TFS showed to increase the heat deflection temperature by as much as 196% over the neat matrix. TSFH showed an increase as much as 162% over the neat matrix. TSFH biocomposites displayed lower heat deflection temperatures than the TFS biocomposites; this is likely due to more residual oils on the TSFH.

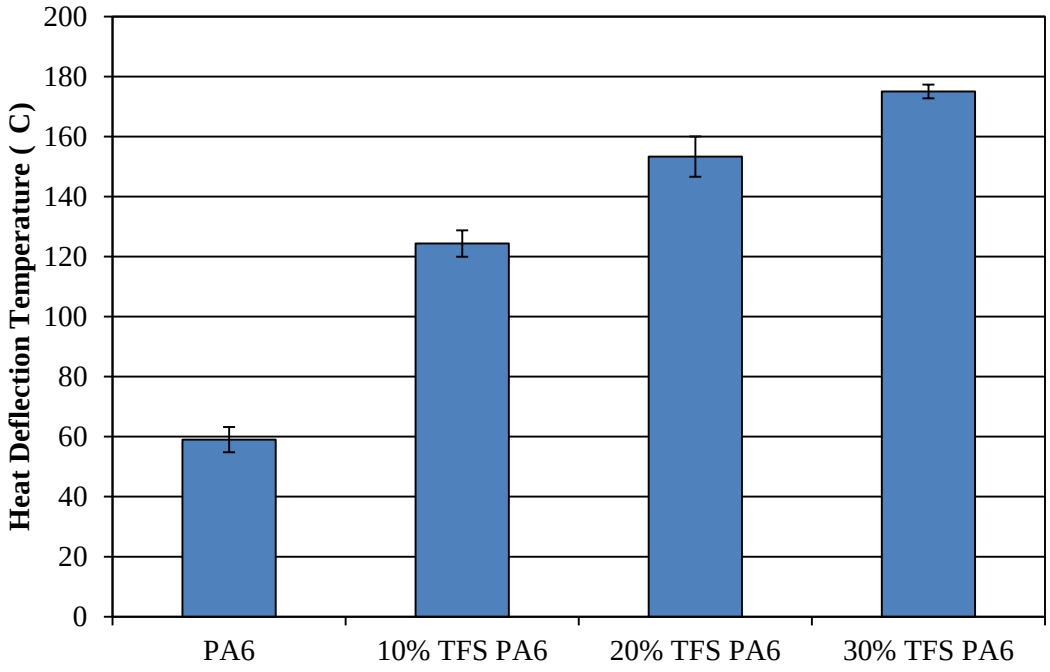

Figure 5.21: Heat deflection temperature of torrefied flax shive reinforced PA6.

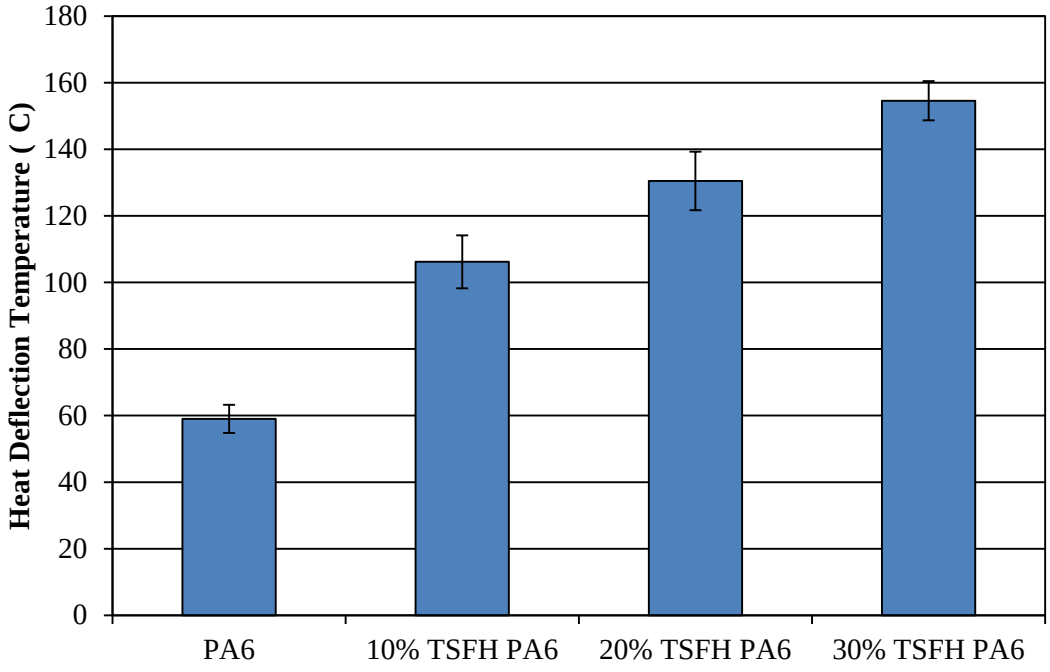

Figure 5.22: Heat deflection temperature of torrefied sunflower hull reinforced PA6.

5.10. Coefficient of Linear Thermal Expansion

Similar to heat deflection temperature, the effects of increased rigidity should hold true for linear thermal expansion. The added fillers restrict the movement of the polymer chains resisting the expansion of the material. Figure 5.23 shows the coefficient of linear thermal expansion for the TFS PA6 biocomposites. The figure shows an increasing and then decreasing trend with increased filler loadings. With the high variation in the neat matrix, no clear difference is present with the added filler. The method with which the coefficients are determined leaves room for human error as well. Figure 5.24 shows the coefficient of linear thermal expansion for the TSFH PA6 biocomposites. Again no clear trend was observed. Both TFS and TSFH displayed similar coefficients of linear thermal expansion.

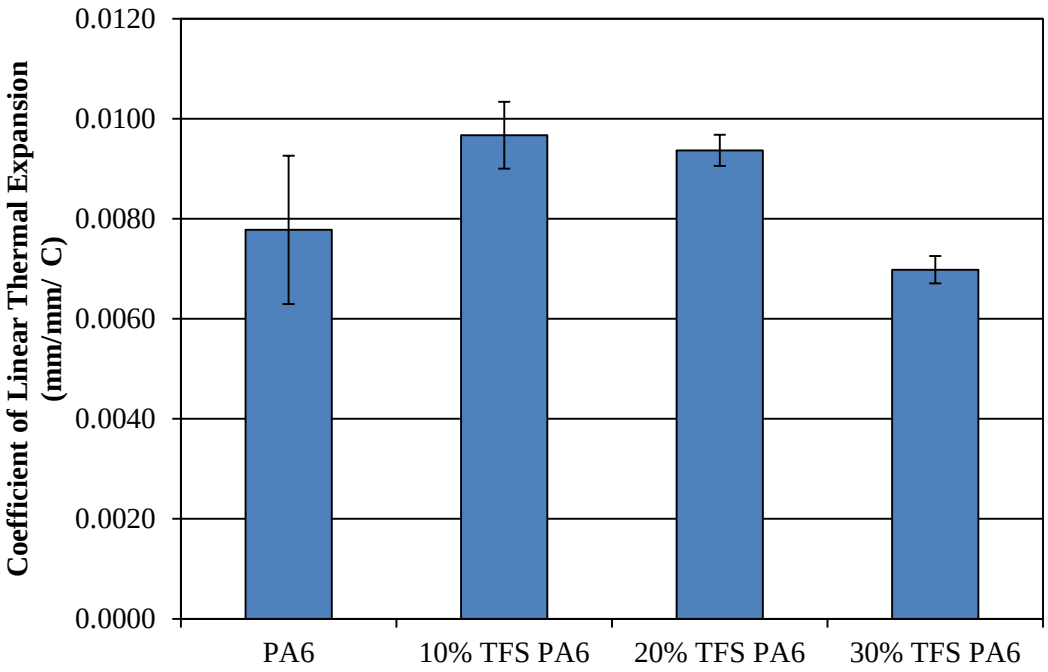

Figure 5.23: Coefficient of linear thermal expansion of torrefied sunflower hull reinforced PA6.

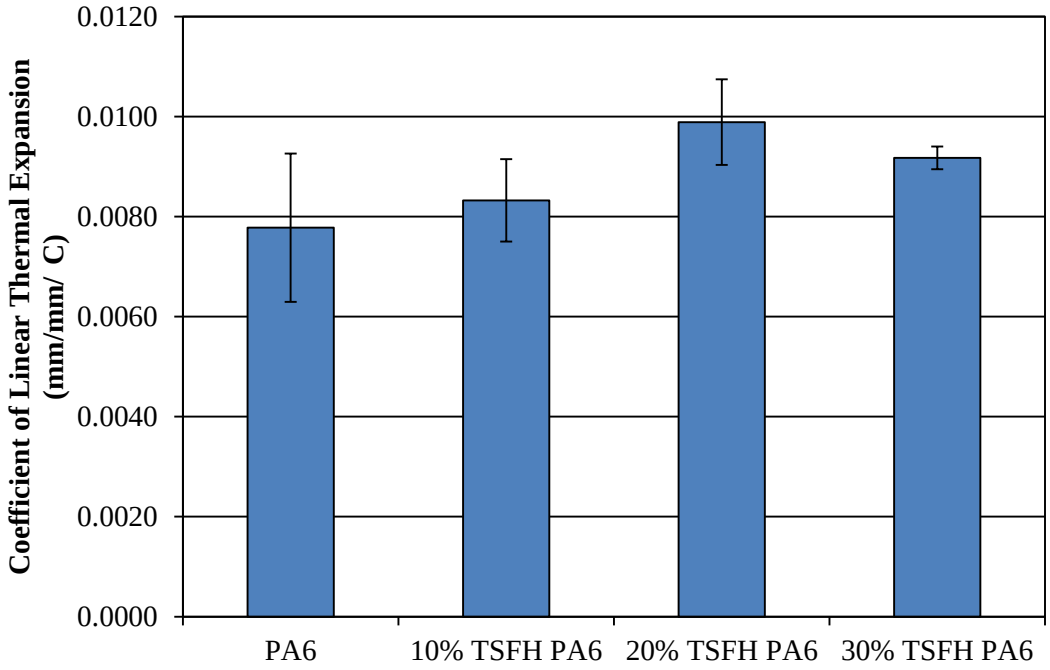

Figure 5.24: Coefficient of linear thermal expansion of torrefied flax shive reinforced PA6.

5.11. Melt Flow Index

Melt flow index is a measure of how easily a polymer flows through an orifice in the molten state. It is also an indirect measurement of molecular weight of a material; a higher melt flow index correlates to a lower molecular weight. Figure 5.25 and Figure 5.26 show the measured melt flow indexes for the torrefied biomass reinforced polyamides. It should be noted here the neat matrix had such a low viscosity it could not be measured, all the molten polymer exited the barrel very quickly upon load application. Both TFS and TSFH produced lower melt flow indexes from the neat matrix, thus indicating higher molecular weight than the neat matrix. It is interesting that TSFH showed an increasing melt flow index with increased filler loading, when increased filler loadings generally increase the viscosity of composites. TFS showed a similar trend to the TSFH. This inverse trend leads

to further evidence the torrefaction may not have been complete as the degradation of the biomass can act as a plasticizer. With increased filler loading there is an increased amount of effective plasticizer, thus an increase in melt flow index. Residuals oils on the fiber surface may have potentially played a role in the inverted melt flow index trends; increased oil content due to increased fiber loading created more lubrication for polymer chain movement. As sunflower hulls contain more oil than flax shive, this explains the enhanced effect in the TSFH reinforced biocomposites. It is possibly this residual oil explains the interesting results in tensile and flexural testing.

5.12. Microscopy

The investigation of the mechanical performance of torrefied biomass reinforced polyamides uncovered some evidence of voids present in the materials. To evaluate which of the materials contained voids, optical microscopy was used. Figures 5.27-5.35 show microscopy images taken of each of the biocomposites grades. Figure 5.27 shows the neat matrix which is void free. If voids had been present in the neat matrix this would have indicated moisture within the material. The lack of voids indicates the drying time prior to injection molding was sufficient to drive off any moisture from storage. The lack of voids also indicates the molding parameters such as temperature and pressure were correctly chosen for the given application.

Figure 5.28 shows an image taken from a 10 wt% TFS specimen. The dispersion of fibers looks to be very even. The fiber particles although smaller than the starting material do appear to have maintained some aspect ratio throughout the processing. Over the entire specimen, no voids were found.

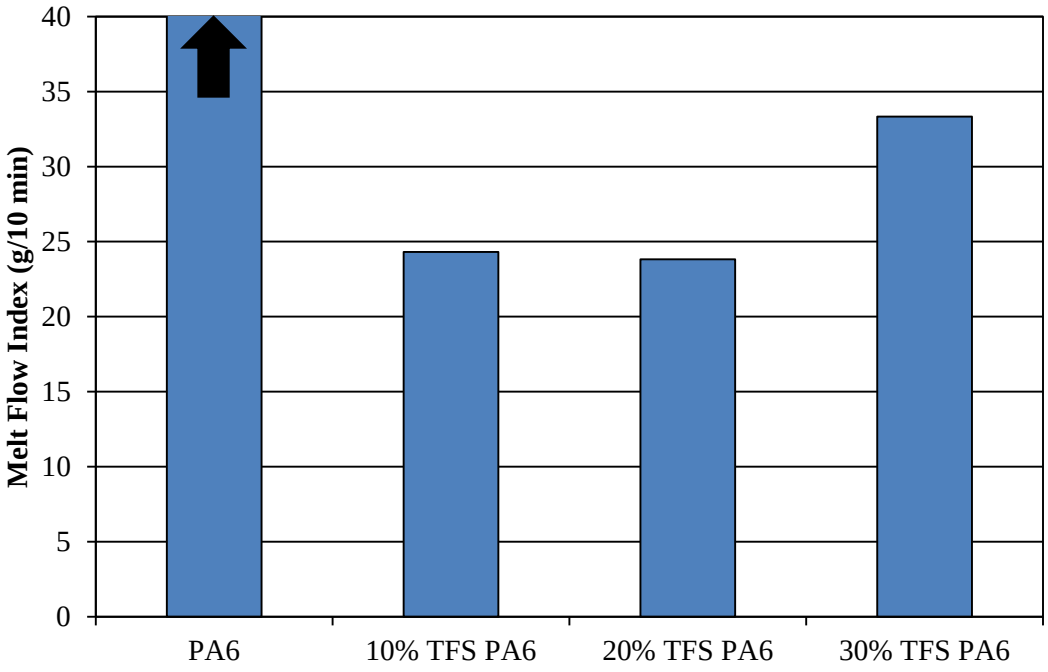

Figure 5.25: Melt flow indexes for torrefied flax shive reinforced PA6.

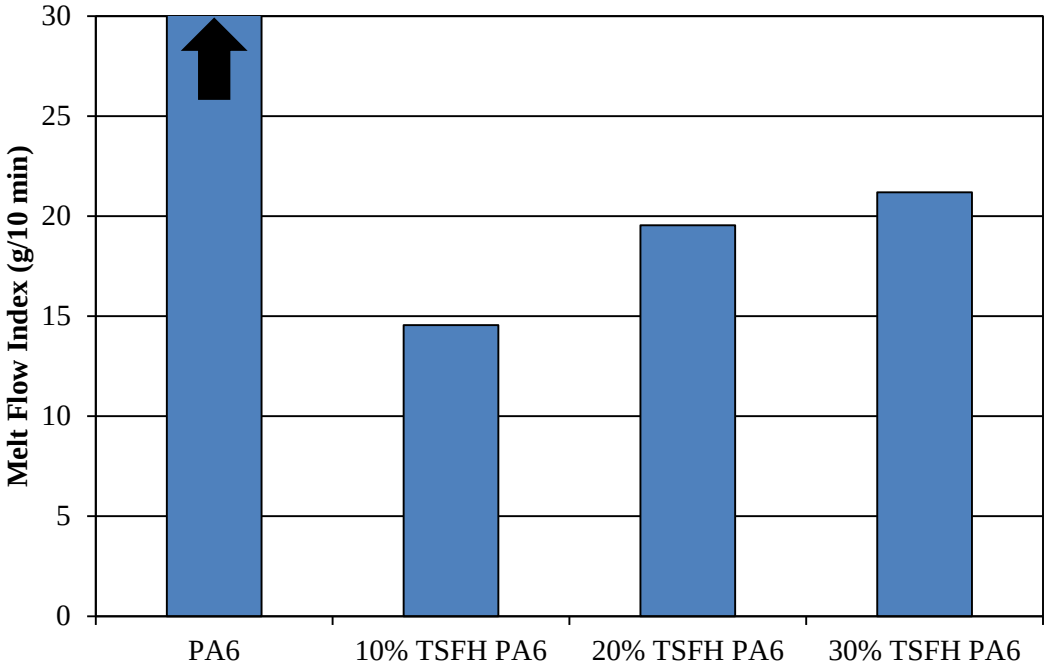

Figure 5.26: Melt flow indexes for torrefied sunflower hull reinforced PA6.

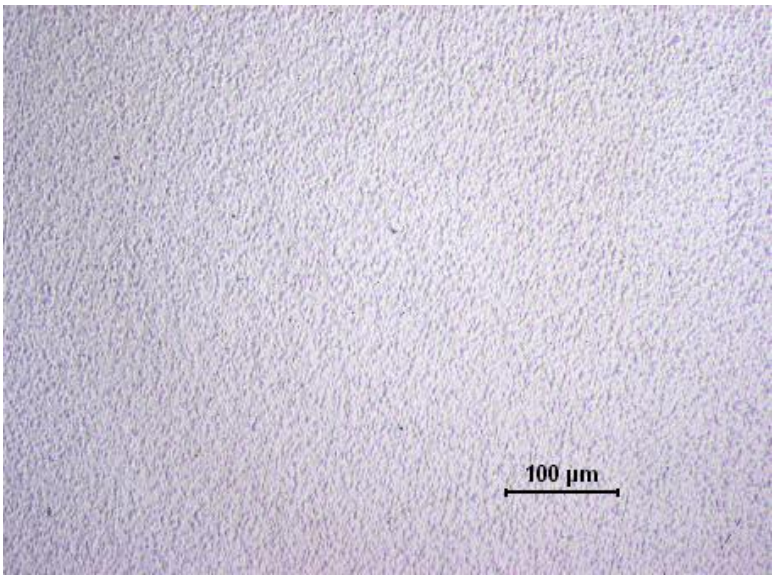

Figure 5.27: 20X microscopy image of neat PA6.

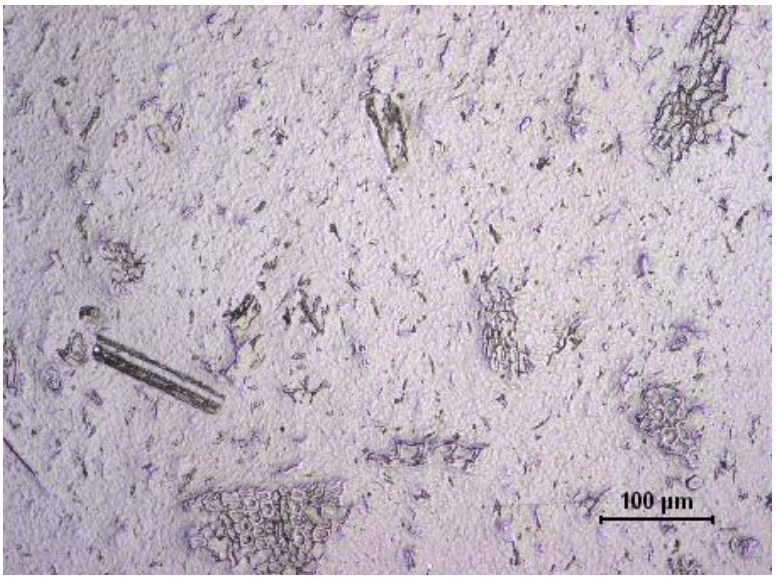

Figure 5.28: 20X microscopy image of 10 wt% TFS in PA6.

Figure 5.29 shows an image taken from a 20 wt% TFS specimen. In the figure an approximately 100 µm diameter void can be seen. This confirms the suspicion from mechanical testing that voids were present in the material. Very few voids were found in the entire specimen examined however. Figure 5.30 shows another image taken of the same

specimen. The majority of the specimen resembled this figure. The fiber dispersion is good and some aspect ratio remains, approximately 2:1 to 5:1 length to width.

Figure 5.31 shows a void ridden section of a 30 wt% TFS specimen. Again the mechanical results discussed earlier indicated some voids may be present in the molded specimens. The large void in the middle is approximately 300 μm in diameter. These voids were found scattered throughout the specimens with some voids being visible with the naked eye. Figure 5.32 shows an image form a non-void ridden section of the same specimen. Fiber dispersion and fiber aspect ratio appear to be very similar to the other TFS specimens.

Figure 5.33 shows an image taken from a 10 wt% TSFH specimen. The entire specimen was examined under microscopy and no voids were found present in the sample. The image shows good dispersion of the fibers and it shows a range of aspect ratios within the fibers; ranging from approximately 3:1 to 4:1 length to width. The fibers for this work were not ground to a specific sieve size but they were coarsely ground in a household coffee grinder to reduce the size some prior to extrusion. As the average particle has an aspect ratio of 3:1 going into the extrusion process it is clear from the image the extrusion and injection molding processes did fractionate the fiber further. It is interesting to note the larger fibers in the upper left corner of the image; this shows that some aspect ratio is retained by not grinding the fiber prior to composite production.

Figure 5.34 shows an image taken from a 20 wt% TSFH specimen. Once again the entire specimen being examined was void free. The fiber show good dispersion throughout the specimen. Once again there is indication of some aspect ratio surviving the composite

processing. The large fiber on the left hand side of the image has maintained an aspect ratio of approximately 3:1, that being the same as that of the fibers prior to processing.

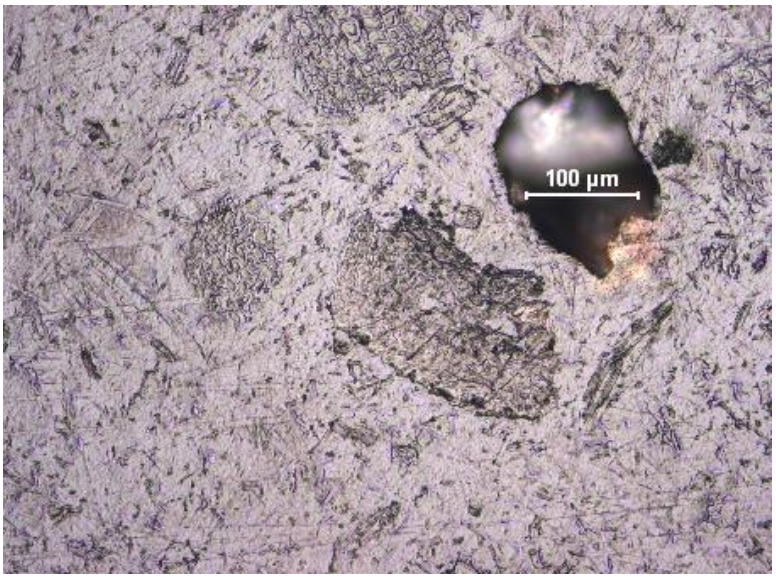

Figure 5.29: 20X microscopy image of void found in 20 wt% TFS in PA6.

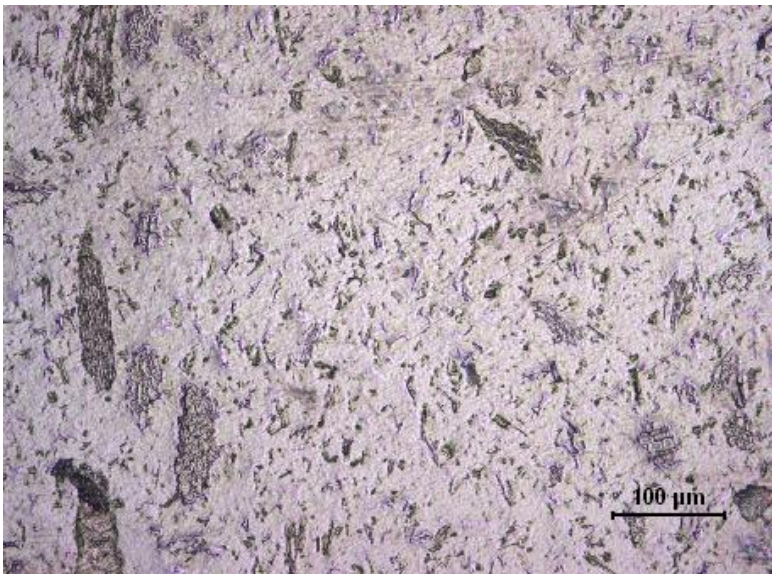

Figure 5.30: 20X microscopy image of 20 wt% TFS in PA6.

Figure 5.35 is the image taken from a 30 wt% TSFH specimen. The fiber density has increased as is expected with increased filler loading and once again there appears to be an even dispersion within the matrix. No voids were found in this specimen either. The larger

particles on the right side of the image again indicate some aspect ratio is maintained throughout the processing of the composites.

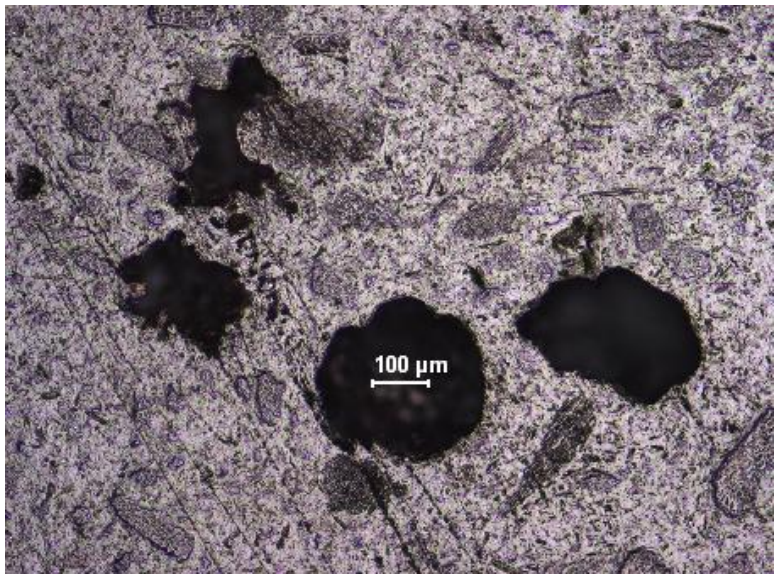

Figure 5.31: 10X microscopy image of voids found in 30 wt% TFS in PA6.

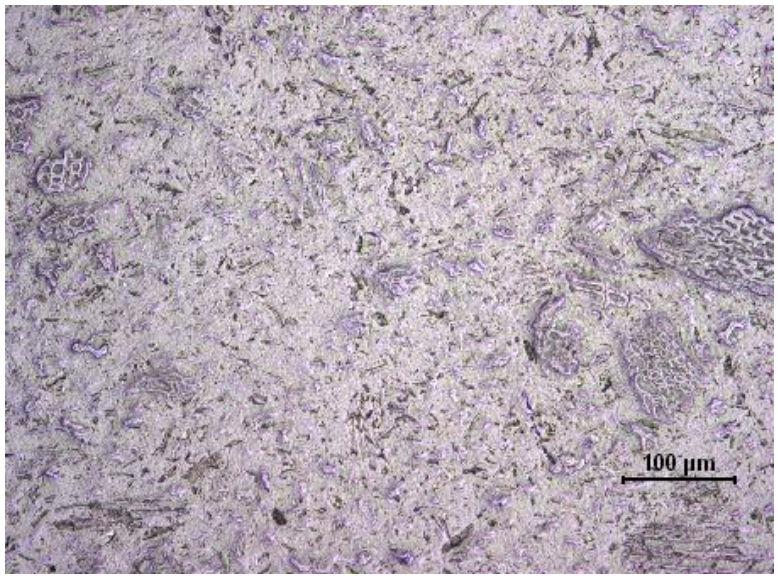

Figure 5.32: 20X microscopy image of 30 wt% TFS in PA6.

The TSFH specimens all showed to be void free indicating the torrefaction of the sunflower hulls may have been more successful than the flax shive. Even though no voids were found in the specimens, the discrepancies in mechanical property trends from the

literature does indicate that some degradation of the filler is still occurring during processing. This likely could be elevated by a torrefaction process that yields more homogenous and consistent results.

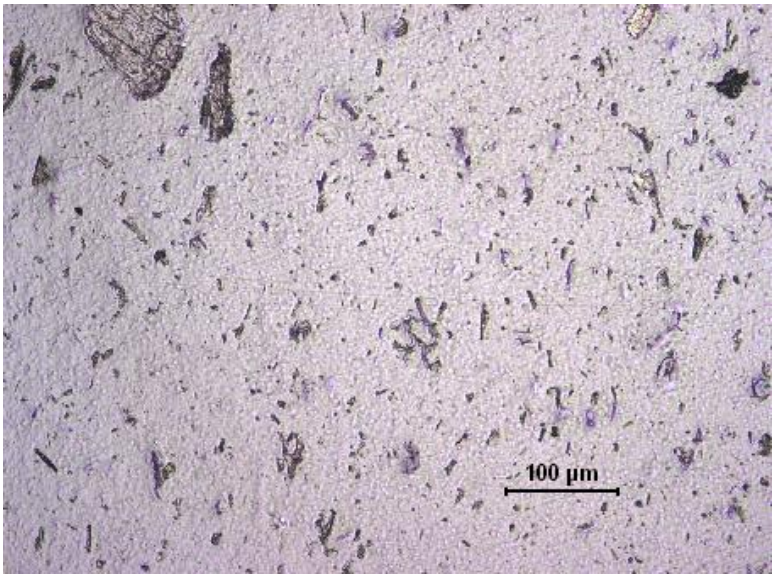

Figure 5.33: 20X microscopy image of 10 wt% TSFH in PA6.

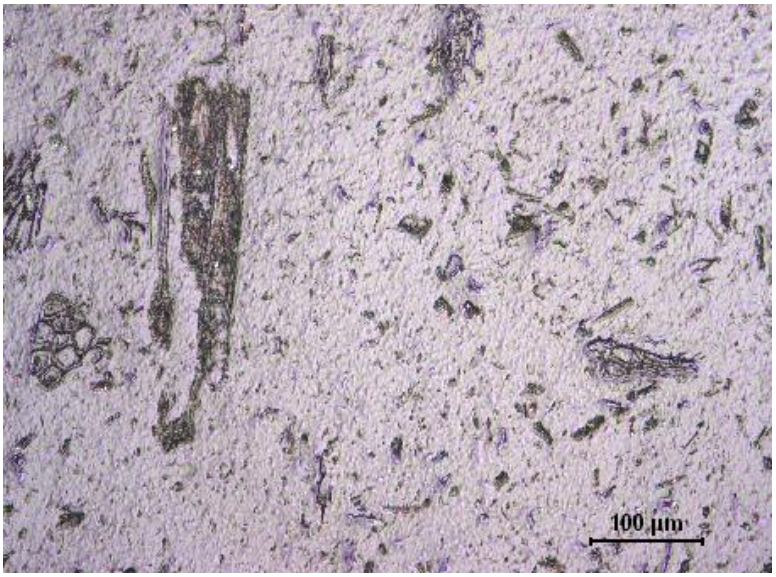

Figure 5.34: 20X microscopy image of 20 wt% TSFH in PA6.

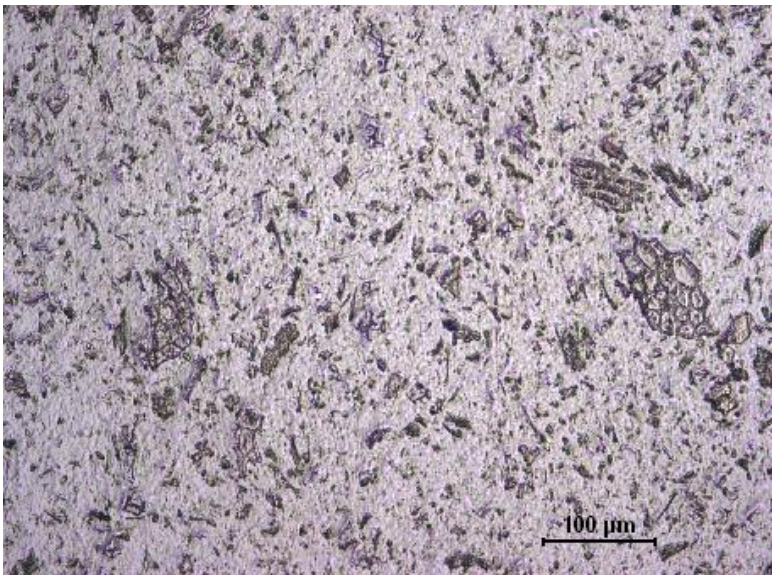

Figure 5.35: 20X microscopy image of 30 wt% TSFH in PA6.

CHAPTER 6. CONCLUSIONS AND RECOMMENDATIONS

Through the torrefaction of flax shive and sunflower hulls, polyamide biocomposites have been successfully produced. By converting the hemicellulose, fats, waxes, et cetera that degrade at a lower temperatures, a biomass filler has been created that can withstand the increased processing temperatures of PA6. PA66 blends were also produced but the processing temperatures proved to still be too detrimental to the filler. The lack of a consistent and uniform torrefaction process lead to the failure of producing good quality PA66 biocomposites in this study.

Torrefied flax shive was shown to improve the elastic modulus of PA6 while maintaining similar tensile strengths. Flexural properties were also improved with increased filler loading. As would be expected, the impact toughness of torrefied flax shive reinforced PA6 saw some decrease from the neat matrix. However, this decrease in impact toughness was not as dramatic as those seen in polyolefin biocomposites. Melt strength and viscosity were greatly improved with the addition of torrefied flax shive. The dynamic mechanical properties of heat deflection temperature and storage modulus all saw increasing trends with increased filler loading, surpassing the performance of the neat matrix. The glass transition temperature was maintained. Density results indicated the specimens contained voids and this was confirmed with microscopy analysis. The voids within the molded specimens give some indication that the torrefaction process was not complete or uniform.

Torrefied sunflower hulls were shown to increase the elastic modulus of the neat PA6, while maintaining a tensile strength similar to that of the neat polymer. Flexural

properties were maintained or improved upon the neat matrix, with some loss in impact toughness. Thermal mechanical properties of the neat matrix were improved with the addition of torrefied sunflower hulls. The melt strength and viscosity were also increased as was heat deflection temperature. Glass transition temperature saw minor decreases from the neat matrix while the storage modulus was shown to increase over the neat matrix above the glass transition temperature. Microscopy images showed the specimens were clear of voids. The specimens being void free were an indication that the torrefaction of the sunflower hulls was more successful than that of the flax shive.

In general the incorporation of torrefied biomass has shown to improve the heat deflection temperature, moisture resistance, and lowered the coefficient of linear thermal expansion, while maintaining the strength of the neat polyamide. These property changes make torrefied biomass filled biocomposites appealing for under the hood applications where components are exposed to elevated temperatures and humidity. It is critical for these under the hood components to maintain mechanical and physical integrity during the life of a vehicle. The utilization of torrefied biomass reinforced biocomposites does require some design considerations. Figure 6.1 shows several handles molded using neat polyamide and torrefied reinforced polyamide. This image shows the difference in final part dimensions when torrefied filler is added as well as how the surface quality changes. To accommodate the decreased mold shrinkage with torrefied biomass biocomposites tooling for existing molded parts would need to be re-tooled to ensure dimensional tolerances are maintained. Furthermore, to improve the surface quality of the biocomposite parts, mold heaters would need to be utilized. With the addition of torrefied biomass, cooling rates are increased resulting in skin formation at the flow front.

Figure 6.1: Molded final products made from neat polyamide (left) and torrefied biomass reinforced polyamide (center).

While this is a good start to solving the problem of introducing natural fibers into engineering thermoplastics, there is a long ways to go. This study has looked at one method of torrefaction that is very energy and time intensive. One goal of biocomposites is to reduce the dependence on petroleum; however another goal is to reduce the cost of materials for the end user. As the method of torrefaction used for this work is energy intensive, the cost benefit is likely not there at this time. One task moving forward with this project is to determine the economics of this method while attempting alternate, less energy intensive, torrefaction methods.

Other goals moving forward with this work would be to first replicate the results produced in this work or to improve upon them. If a more uniform consistent process could be implemented the properties indicated in literature could potentially be achieved. Some further investigation is needed to really determine why the flax shive filled biocomposites were void ridden at higher loadings. As was stated before it could have been due to incomplete torrefaction, however if further analysis reveals the torrefaction process was

successful, other phenomena need to be explored. Some of the other inconsistent mechanical and physical results, such as the moisture absorption results for torrefied sunflower hulls, need to be explored more.

With the ever increasing use of biocomposites in everyday goods, it is imperative to explore a wide range of base matrices. It has been shown that torrefied biomass improves the storage characteristics of the mass; this could potential lead to a longer end user life for biocomposites as well, especially in biodegradable systems. It would be worthwhile to investigate the use of torrefied fillers in biodegradable systems to see how it effects their life cycle. As biomass feedstock is hard to justify transporting any distance, the exploration of various feedstocks from around the globe need to study for greater acceptance of this technology.

REFERENCES

[1] E. McHenry and Z. H. Stachurski, “Composite materials based on wood and nylon fibre,” *Composites Part A: Applied Science and Manufacturing*, vol. 34, no. 2, pp. 171–181, Feb. 2003.

[2] G. Sui, M. a Fuqua, C. a Ulven, and W. H. Zhong, “A plant fiber reinforced polymer composite prepared by a twin-screw extruder.,” *Bioresource technology*, vol. 100, no. 3, pp. 1246–51, Feb. 2009.

[3] P. Santos, M. Spinace, K. Fermoselli, and M. Depaoli, “Polyamide-6/vegetal fiber composite prepared by extrusion and injection molding,” *Composites Part A: Applied Science and Manufacturing*, vol. 38, no. 12, pp. 2404–2411, Dec. 2007.

[4] D. Bruce, R. Hobson, J. Farrent, and D. Hepworth, “High-performance composites from low-cost plant primary cell walls,” *Composites Part A: Applied Science and Manufacturing*, vol. 36, no. 11, pp. 1486–1493, Nov. 2005.

[5] M. A. Fuqua and C. A. Ulven, “Characterization of Polypropylene/Corn Fiber Composites with Maleic Anhydride Grafted Polypropylene,” *Journal of Biobased Materials and Bioenergy*, vol. 2, no. 3, pp. 258–263, Sep. 2008.

[6] M. Avella, M. Malinconico, A. Buzarovska, A. Grozdanov, G. Gentile, and M. E. Errico, “Natural Fiber Eco-Composites,” *Polymer Composites*, vol. 28, no. 1, pp. 98–107, 2007.

[7] V. S. Chevali, M. A. Fuqua, S. Huo, and C. A. Ulven, "Utilization of Agricultural By-products as Fillers and Reinforcements in ABS," *SAE International Journal of Materials & Manufacturing*, vol. 3, no. 1, pp. 221–229, 2010.

[8] R. N. Rothon, Ed., *Particulate-Filled Polymer Composites*, 2nd ed. Rapra Technology Limited, 2003.

[9] M. Chanda and S. K. Roy, *Industrial Polymers, Specialty Polymers, and Their Applications*. CRC Press, 2009, p. 432.

[10] D. K. Platt, *Engineering and High Performance Plastics Market Report*. A Rapra Market Report, 2003, p. 188.

[11] E. Carlson and K. Nelson, "Nylon Under the Hood: A History of Innovation," vol. December. DuPont, 2003.

[12] W.-H. Chen and P.-C. Kuo, "Torrefaction and co-torrefaction characterization of hemicellulose, cellulose and lignin as well as torrefaction of some basic constituents in biomass," *Energy*, vol. 36, no. 2, pp. 803–811, Feb. 2011.

[13] N. S. Murthy, "Hydrogen Bonding, Mobility, and Structural Transitions in Aliphatic Polyamides," *Journal of Polymer Science: Part B: Polymer Physics*, vol. 44, pp. 1763–1782, 2006.

[14] R. M. Rowell, "Chemical modification of wood: A short review," *Wood Material Science and Engineering*, vol. 1, no. 1, pp. 29–33, Mar. 2006.

[15] R. E. Ibach and C. M. Clemons, “Effect of Acetylated Wood Flour or Coupling Agent on Moisture , UV , and Biological Resistance of Extruded Woodfiber-Plastic Composites,” in *Wood Protection*, 2006, pp. 139–147.

[16] K. Segerholm, “Wood Plastic Composites made from Modified Wood - Aspects on Moisture Sorption, Micromophology, and Durability,” KTH Architecture and the Built Environment, 2007.

[17] S. Galland, “Microstructure and Micromechanical Studies of Injection Moulded Chemically Modified Woor/Poly(lactic acid) Composites,” Lulea University of Technology, 2009.

[18] H. P. S. A. Khalil, H. Ismail, H. D. Rozman, and M. N. Ahmad, “The effect of acetylation on interfacial shear strength between plant fibres and various matrices,” *European Polymer Journal*, vol. 37, pp. 1037–1045, 2001.

[19] J. Follrich, U. Muller, W. Gindl, and N. Mundigler, “Effects of Long-term Storage on the Mechanical Characteristics of Wood Plastic Composites Produced from Thermally Modified Wood Fibers,” *Journal of Thermoplastic Composite Materials*, vol. 23, no. 6, pp. 845–853, May 2010.

[20] W.-H. Chen and P.-C. Kuo, “A study on torrefaction of various biomass materials and its impact on lignocellulosic structure simulated by a thermogravimetry,” *Energy*, vol. 35, no. 6, pp. 2580–2586, Jun. 2010.

[21] M. Keiluweit, P. S. Nico, M. G. Johnson, and M. Kleber, “Dynamic molecular structure of plant biomass-derived black carbon (biochar).,” *Environmental science & technology*, vol. 44, no. 4, pp. 1247–53, Feb. 2010.

[22] J. J. Chew and V. Doshi, “Recent advances in biomass pretreatment – Torrefaction fundamentals and technology,” *Renewable and Sustainable Energy Reviews*, vol. 15, no. 8, pp. 4212–4222, Oct. 2011.

[23] T. Bridgeman, J. Jones, I. Shield, and P. Williams, “Torrefaction of reed canary grass, wheat straw and willow to enhance solid fuel qualities and combustion properties,” *Fuel*, vol. 87, no. 6, pp. 844–856, May 2008.

[24] M. Prins, K. Ptasinski, and F. Janssen, “Torrefaction of woodPart 1. Weight loss kinetics,” *Journal of Analytical and Applied Pyrolysis*, vol. 77, no. 1, pp. 28–34, Aug. 2006.

[25] M. Prins, K. Ptasinski, and F. Janssen, “Torrefaction of woodPart 2. Analysis of products,” *Journal of Analytical and Applied Pyrolysis*, vol. 77, no. 1, pp. 35–40, Aug. 2006.

[26] G. Lardy and V. Anderson, “Alternative Feeds for Ruminants,” *AS-1181*, 2009. .

[27] D. E. Akin, J. a Foulk, R. B. Dodd, and D. D. McAlister, “Enzyme-retting of flax and characterization of processed fibers.,” *Journal of biotechnology*, vol. 89, no. 2–3, pp. 193–203, Aug. 2001.

[28] M. A. Fuqua, “Mechanical Modeling of Thermoplastics Reinforced with Biobased Particulate,” North Dakota State UNiversity, 2011.